NASA Contractor Report 170408

NASA-CR-170408
19840006922

A Preliminary Investigation of the Drag and Ventilation Characteristics of Livestock Haulers

J. A. Hoffman and D. R. Sandlin

Contract NAG4-7
December 1983

National Aeronautics and
Space Administration

NASA Contractor Report 170408

A Preliminary Investigation of the Drag and Ventilation Characteristics of Livestock Haulers

J. A. Hoffman and D. R. Sandlin
California Polytechnic State University, San Luis Obispo, California 93407

Prepared for
Ames Research Center
Dryden Flight Research Facility
Edwards, California
under Contract NAS4-7

1983

National Aeronautics and
Space Administration
Ames Research Center
Dryden Flight Research Facility
Edwards, California 93523

Use of trade names or names of manufacturers in this report does not constitute an official endorsement of such products or manufacturers, either expressed or implied, by the National Aeronautics and Space Administration.

ABSTRACT

A wind tunnel evaluation of the drag and ventilation characteristics of a conventional (unmodified) and five modified subscale model livestock haulers at 0°yaw angle has been made. The unmodified livestock hauler has a relatively high drag coefficient, and a low velocity recirculation region exists in the forward portion of the hauler. The use of a streamlined forebody and enclosed gap reduced the drag coefficient of one model by 42% and improved the rate at which contaminants can be flushed from the cargo compartment by a factor of 2.5. From the limited data obtained, any increase in the fraction of open area of the trailer sides was found to improve the trailer ventilation. The use of a ram air inlet can improve the ventilation within the hauler and remove the low velocity recirculation region at the expense of a modest increase in the truck's drag coefficient. A mathematical model for vehicles with ram air or NACA submerged inlets was developed and appears to adequately predict the ventilation characteristics of livestock haulers. In a limited study, the wind tunnel model flow patterns for an unmodified configuration appear to correspond favorably to full-scale results of an unmodified vehicle.

NOMENCLATURE

Symbols

A	Area
A_b	Total area of trailer tailgate surface, base
A_{3b}	Total open area of trailer base
A_M	Total open area of manifold at discharge (see Figs. 34 & 35)
A_p	Projected truck area
A_{3s}	Total open area of trailer sides
A_3	Total open area of trailer, tailgate and sides, $= A_{3b} + A_{3s}$
A_{ts}	Total area of trailer sides
C_d	Coefficient of discharge
C_D	Coefficient of drag, $= D/\rho\ V_\infty^2\ A_p/2$
C_M	Static pressure loss coefficient of air distribution manifold, $= (P_2 - P_h)\ /\ \rho V_2^2/2$
C_{Ph}	Dimensionless hauler pressure, $= (P_h - P_\infty)/\ \rho V_\infty^2/2$
C_{Pd}	Static pressure recovery coefficient of inlet diffuser, $= (P_2 - P_1)/\ \rho V_1^2/2$
C_{Pe}	Dimensionless static pressure on exterior of vehicle, $= (P_e - P_\infty)/\ \rho V_\infty^2/2$
C_{Po}	Dimensionless static pressure at entrance, $= (P_o - P_\infty)/\ \rho V_\infty^2/2$
C_{P3}	Dimensionless static pressure at discharge, $= (P_3 - P_\infty)/\ \rho V_\infty^2/2$
C_Q	Dimensionless theoretical flow coefficient through hauler, $= A_3V_3/A_1V_\infty$
D_h	Hydraulic diameter
G	Gap dimension between tractor and trailer
H	Height

K	Total pressure loss coefficient
L	Length
N_V	Ventilation effectiveness, the ratio of the theoretical to the actual ventilation times
P	Static pressure
R_e	Reynolds number based on vehicle length, $V_\infty L_V/\nu$
RRR	Ram recovery ratio
t	Measured ventilation time
T	Dimensionless ventilation parameter, $= V_\infty t/L_t$
V	Velocity
W	Width
θ	Discharge angle of fluid from manifold
ρ	Fluid density
η_d	Diffuser efficiency
ν	Kinematic viscosity

Subscripts

o	Free-stream adjacent to vehicle at inlet of Ram air or NACA entrance
1	Ram air or NACA submerged entrance throat (minimum area) location
2	Diffuser exit location
3	Hauler discharge location
4	Downstream end of manifold (See Fig. 35)
∞	Freestream upstream of vehicle
c	Cab or tractor
d	Diffuser

E	Entrance
h	Hauler
M	Manifold
t	Trailer
v	Vehicle

Note: 1) The primary criteria for defining the ventilation characteristics in this report are the dimensionless ventilation parameter, T, and visual observations of the flow. In the case for the full-scale unmodified vehicle, "Model B", some local measurements of flow velocity were made in conjunction with flow direction observations.

2) The following definitions apply to data and discussions about the tailgate or trailer base region.

tailgate open, $A_{3b}=A_b$, vented

tailgate closed, $A_{3b}=0$, unvented

TABLE OF CONTENTS

LIST OF TABLES

LIST OF FIGURES

INTRODUCTION

The National Cattlemen's Association considers the leading cause of livestock loss to be Bovine Respiratory Disease (1). The environment that livestock are subject to during shipping is a major contributing factor to the cause of this disease. The most common mode of transportation of livestock is the tractor-trailer combination. Livestock are loaded into the trailer using a high density load factor and are transported to their destination. The period of time that the livestock spend in the trailer can be extensive and the trailer environment is usually uncomfortable and, in many cases, life endangering. Overheating, uneven ventilation, and unfavorable air composition (dust and fumes due to ingestion and animal-generated moisture and ammonia vapor) exist. The livestock are under a great deal of stress due to a change in environment and daily routines and because calves are separated from their mothers. The livestock are subjected to fatigue caused by long hours of travel in cramped quarters. The result is that 3% to 5% of the cattle die while enroute or shortly after arrival; this loss has been attributed to Bovine Respiratory Disease, sometimes called 'shipping fever.'

Bovine Respiratory Disease is highly complex and not completely understood. Many facets of the disease are influenced by geography, season, transportation time and weather, nutrition, stress due to shipping environment, presence of bacteria and viral organisms and other factors. A limited literature survey has been made to learn more about this disease, the effect caused by the transportation of animals in tractor-trailer vehicles for long distances, and suitable ventilation requirements. The search to define ventilation requirements for livestock has not produced satisfactory results.

It appears that limited research has been directed towards this end. Such bioclimatic factors as air composition, humidity, air temperature and air movement are important. Of course, enough free air must be provided to satisfy the breathing requirements for a cow, which is approximately .113 m^3/min. (4 ft^3/min) for a standing and resting cow. This quantity increases five times as the temperature increases from 10°C to 40.5°C (50°F to 105°F) (2). The rate of change of room air must be great enough to provide free air to breathe and to control the concentration of certain gases and odors. The movement of air also produces wind-chill; a wind-chill chart developed by the U.S. Army for man, which should be applicable to animals, is presented in reference (3). The ideal environmental temperature for various livestock are presented by ASHRAE (4).

The rapid increase in the cost of fuel has prompted new interest in research to improve the aerodynamic efficiency of ground vehicles. The reduction of aerodynamic drag results in improved fuel efficiency. The objective of much of this research is the altering of the air flow patterns over the vehicles so that smooth attached flow is obtained. The change of flow over the vehicles is achieved either by altering the design of the vehicles, or by adding devices to the existing design, or a combination of the two. Muirhead (5) has estimated that between 4.2×10^9 and 8.3×10^9 liters of fuel per year could be saved if the entire U.S. fleet of tractor-trailer vehicles were redesigned for aerodynamic efficiency; this corresponds to a saving of between 1.7 and 3.4 percent of the nation's annual imported crude oil for the import rates of the mid 1970's.

In a study of the drag of tractor-trailer vehicles, Marks (6) found that at 0^o yaw less than 15% of the vehicle drag was caused by base drag (drag

attributable to flow separation at the rear of the trailer) and concluded that most of the tractor-trailer drag was due to forebody drag (caused by flow separation on the front surface of the tractor-trailer). He found that rounding the leading vertical edges of the trailer decreased the drag coefficient at zero yaw by 15.9%. Saltzman (7) obtained a 40% reduction in the drag coefficient of a single box-shaped ground vehicle by rounding the vertical corners.

In a study of the drag of two sharp-edged, axisymmetrical bodies located perpendicular to the flow and in tandem, Roshko (8) found an optimum gap for a minimum drag; the optimum gap and minimum drag coefficients were both functions of the size ratio of the two bodies. Mason (9) and Buckley (10) found, in the range of gap ratios studied, that the drag coefficient of tractor-trailer vehicles increased about 35% as the gap between the tractor and trailer increased. Add-on devices such as vanes, lips, fairings, boat-tails, and underbody treatments have been studied by many authors. Marks (11) found that vanes located on the front-vertical edges of a cab-over-engine tractor reduced the drag coefficient of the tractor-trailer by as much as 10.4%; vanes located at other locations on the tractor and trailer had less effect. Lissaman (12) found that a lip, a rounded horizontal corner on the front-top leading edge of a truck, resulted in about a 35% reduction in the drag coefficient of the single chassis, full-scale truck. Kirsch (13) obtained a 27% decrease in the drag coefficient of a van with sharp corners when vanes were attached to the front-top edge and the front-side edges. Mason (9) found that a fairing attached to the top of the tractor decreased the drag coefficient of a tractor-trailer vehicle between 20 and 30%; the decrease in drag coefficient was dependent upon the gap between the tractor

and trailer. Studies by Muirhead (5) (14) showed that the drag coefficient of a typical cab over-engine tractor-trailer vehicle could be reduced from 0.99 for the unmodified vehicle to 0.40 by rounding the cab nose and top, enclosing the gap between the tractor and trailer, lowering the side panels, and using a boat-tail and a smooth bottom; the reduction in the drag coefficient for each modification was evaluated.

In the case of livestock haulers, there is some question as to how the alteration of flow patterns to reduce drag will affect the environment that the livestock are subject to within the trailer. No published information on the ventilation characteristics of livestock haulers has been found. A reasonable question to ask is "Can the environment within a cattle trailer be better controlled or improved for trucks designed for low drag profiles?" In the spring of 1977, Dr. Floyd Horn of the Department of Agriculture's Agricultural Research Service, after review of some of the low drag trucks suggested by the NASA/Dryden Flight Research Facility (DFRF), asked how flow changes necessary for low drag would alter the environment within a livestock trailer and asked if the closed forebody used by DFRF to reduce drag could cause severe overheating of the animals. The DFRF responded by pointing out that the closed and rounded forebody promotes attached flow which should provide the opportunity to control the ingestion and exhaust of air thereby reducing the heating and improve the ventilation within the trailer. The heat buildup in livestock trailers is probably aggravated by large separation bubbles along the top and sides of trucks with square corners. These separation bubbles can be avoided by using significant forebody corner radii. A simple forward-facing ram air inlet and/or NACA submerged inlets were suggested for air ingestion in sufficient quantity so that more outward

venting would occur throughout the mid and aft regions of the trailer.

The purpose of the inlets is to provide:

1. A built-in natural air distribution and circulation system, so designed that "dead air" regions will be avoided;
2. Relatively more outflow, instead of recirculating flow, along the mid and aft regions so that the ingestion of dust and traffic fumes will be reduced or eliminated;
3. Sufficient air mass flow to carry away the animal-generated moisture and ammonia vapors as they are produced; and
4. The potential for distributing heated air for transport of animals during the cold seasons. Flapper doors or sliding panels could be used to modify the mass flow so as to adjust for differences caused by weather and seasons.

Preliminary wind tunnel tests of sub-scale model livestock haulers have been made to evaluate the ventilation and drag characteristics of models with and without forward facing ram air inlets and/or NACA flush submerged inlets to improve ventilation. In addition, a limited test of an actual full scale livestock hauler has been made.

The purpose of this investigation is to determine for an unmodified and several models modified with forward facing ram air and/or NACA submerged inlet configurations:

1. The circulation patterns within the hauling volume.
2. A relative measure of the air change times.
3. The external pressure distribution on the top and sides of the models.

4. The effect of the vehicle modification on the total drag of the vehicle.

In addition, a mathematical model for the natural ventilation of a moving vehicle and the results of preliminary tests of the circulation of the air within the hauling volume of a full-scale typical livestock hauler is presented.

MATHEMATICAL MODEL FOR THE NATURAL VENTILATION CHARACTERISTICS OF A MOVING VEHICLE

The design of present day livestock haulers results in considerable recirculation of gases within the hauler. Haulers which would allow good (uniform) ventilation characteristics with low recirculation at all hauler speeds could utilize fixed area inlets (ram air or NACA submerged), a variable area design (A_1 and/or A_3 vary with V_∞), and/or an augmented ventilation system (e.g., blower driven for use when the forward velocity of the vehicle is low or zero).

In order to aid in the design of a livestock hauler with desirable unaugmented ventilation characteristics, a simple mathematical model for the passive system illustrated in Figure 1 has been developed. The model predicts the dimensionless static pressure within the hauler (C_{p_h}) and the dimensionless flow rate through the hauler (C_Q) as a function of the ratio of the discharge and inlet areas (A_3/A_1), the total pressure loss coefficient of the entrance (K_E), the static pressure recovery coefficient of the inlet diffuser (C_{pd}), the static pressure loss coefficient of the air distribution manifold (C_M), the dimensionless static pressure at the entrance (C_{po}), and at the discharge (C_{p3}) and the total pressure loss coefficient of the discharge (K_3). The governing equations applicable in various regions illustrated in Figure 1 follow.

The free-stream pressures and velocity upstream of the vehicle are P_∞ and V_∞ respectively.

The free-stream conditions adjacent to the vehicle directly upstream of the inlet (station 0) (assuming no total pressure loss between upstream condition and station 0) are presented by equations 1 and 2:

$$P_o = C_{po}\rho V_\infty^2/2 + P_\infty \qquad \text{Eq. 1}$$

$$\rho V_o^2/2 = (1 - C_{po})(\rho V_\infty^2/2) \qquad \text{Eq. 2}$$

Entrance region (station 0 to station 1):

$$P_1 - P_o = \rho(V_o^2 - V_1^2)/2 - K_E\rho V_o^2/2 \qquad \text{Eq. 3}$$

Inlet diffuser (station 1 to station 2):

$$P_2 - P_1 = C_{pd}\rho V_1^2/2 \qquad \text{Eq. 4}$$

Inlet manifold (station 2 to station h):

$$P_h - P_2 = -C_M\rho V_2^2/2 \qquad \text{Eq. 5}$$

The pressure in the hauler (station h) is P_h and the air velocity is assumed to be zero.

Discharge (station h to station 3):

$$P_h - P_3 = (K_3 + 1)\,\rho V_3^2/2 \qquad \text{Eq. 6}$$

Free-stream pressure adjacent to vehicle at discharge (station 3):

$$P_3 = C_{p3}\rho V_\infty^2/2 + P_\infty \qquad \text{Eq. 7}$$

Adding equations 1, 3, 4, and 5 and substituting equation 2:

$$P_h = \rho V_\infty^2/2 + (C_{pd} - 1)\,\rho V_1^2/2 - K_E\rho V_o^2/2 - C_M\rho V_2^2/2 + P_\infty \qquad \text{Eq. 8}$$

Adding equations 6 and 7:

$$P_h = (K_3 + 1)\,\rho V_3^2/2 + C_{p3}\rho V_\infty^2/2 + P_\infty \qquad \text{Eq. 9}$$

Equating equations 8 and 9 and applying the continuity equation

$(A_3V_3 = A_2V_2 = A_1V_1 = A_oV_o)$ and equation 2:

$$\frac{V_3}{V_\infty} = \frac{(1 - C_{p3}) - K_E\,(1 - C_{po})}{K_3 + 1 + \left(\frac{A_3}{A_1}\right)^2 \left[(1 - C_{pd}) + \frac{C_M}{(A_2/A_1)^2}\right]} \qquad \text{Eq. 10}$$

Dividing equation 9 by $\rho V_\infty^2/2$ and using equation 10:

$$C_{p_h} = \frac{P_h - P_\infty}{\rho V_\infty^2/2} = (K_3 + 1)\left(\frac{V_3}{V_\infty}\right)^2 + C_{p3} \qquad \text{Eq. 11}$$

$$= C_{p3} + \frac{(K_3 + 1)\left[(1 - C_{p3}) - K_E\,(1 - C_{po})\right]}{K_3 + 1 + \left(\frac{A_3}{A_1}\right)^2 \left[(1 - C_{pd}) + \frac{C_M}{(A_2/A_1)^2}\right]}$$

From the definition of the flow coefficient and from equation 9:

$$C_Q = \frac{A_3 V_3}{A_1 V_\infty}$$

$$= \frac{(A_3/A_1)\left[(1 - C_{p3}) - K_E(1 - C_{po})\right]^{0.5}}{\left[K_3 + 1 + \left(\frac{A_3}{A_1}\right)^2 \left[(1 - C_{pd}) + \frac{C_M}{(A_2/A_1)^2}\right]\right]^{0.5}} \qquad \text{Eq. 12}$$

In order to obtain values of K_E for the NACA submerged entrance ducts studied by Mossman (15), the following relationships are presented which relate K_E to the parameters used by Mossman, diffuser efficiency (η_d), and the ram recovery ratio (RRR).

$$\eta_d = \frac{P_2 - P_1}{\rho V_1^2/2} + \left(\frac{V_2}{V_1}\right)^2$$

$$RRR = \frac{P_2 - P_o}{\rho V_o^2/2} + \left(\frac{V_2}{V_o}\right)^2$$

Now using equation 3 with the above definitions:

$$K_E = 1 - RRR - \left(\frac{V_1}{V_o}\right)^2 (1 - \eta_d)$$

Mossman found a near constant value of η_d ($\eta_d = 0.91$) and found that the RRR was a function of V_1/V_o and the geometry of the inlet. Values of RRR for two typical inlets are presented as a function of V_1/V_o in Figure 2, and values of K_E are presented in Figure 3. It can be shown that $V_1/V_o = V_3A_3/V_\infty A_1(1 - C_{po})^{0.5})$ by using the continuity equation and equation 2.

Curves of C_{p_h} and C_Q from equations 10 and 11 are presented as a function of A_3/A_1 in Figures 4 and 5 (an iterative solution is required when $K_E \neq 0$) for the following conditions:

Case 1: $C_{p3} = -0.1$, $C_{pd} = 0$, $K_3 = 0$, $K_E = 0$ and $C_M = 0$

This condition could be simulated by using a simple ram air inlet without a diffuser ($C_{pd} = 0$) or manifold ($C_M = 0$) and with well-formed discharge nozzles ($K_3 = 0$) located near the rear of the hauler, where values of C_{p3} are approximately -0.1 at 0^o yaw angle (see Ahmed (16)).

Case 2: $C_{p3} = -0.1$, $C_{pd} = 0.5$, $K_3 = 0$, $K_E = 0$ and $C_M = 0$

This condition would exist with diffused inlet ram air, without a manifold and with well-formed discharge nozzles located in the hauler.

Case 3: $C_{p3} = -1$, $C_{pd} = 0.5$, $K_3 = 0$, $C_{po} = -0.1$, K_E from Figure 3 and $C_M = 0$

This condition could be achieved, for example, by using NACA submerged entrances and diffusers on the sides of the vehicle, and with well-formed discharge nozzles near the top-front of the vehicle where the local $C_{pe} = -1$

(see Ahmed (16)), thereby obtaining an internal backward flow hauler. Case 3a utilizes NACA submerged entrances with a peak RRR of 0.795, while Case 3b utilizes these same entrances with a peak RRR of 0.895.

Case 4: $C_{p3} = -0.1$, $C_{pd} = 0.5$, $K_3 = 1.5$, $K_E = 0$, and $C_M = 0$

This condition could be achieved if the inlet ram air was diffused and with the discharge occurring through orifices located in the hauler (typical of some present-day haulers). A total pressure loss coefficient of 1.5 represents that of an orifice plate.

Case 5: $C_{p3} = -0.1$, $C_{pd} = 0.5$, $K_3 = 1.5$, $C_{po} = -0.1$, K_E from Figure 3 and $C_M = 0$

This condition could be achieved by using NACA submerged entrances with a peak RRR of 0.895 and diffusers located on the top and/or near the front of the vehicle, and with the discharge occurring through orifices located in the hauler.

Case 6: $C_{p3} = -0.1$, $C_{pd} = 0.5$, $K_3 = 1.5$, $K_E = 0$, $C_M = 0.5$ and $A_2/A_1 = 2$

This condition is the same as that of Case 4, except that a manifold is used after the diffuser to distribute the air.

The curves of C_{p_h} vs. A_3/A_1 presented in Figure 4 asymptotically approach C_{p3}, the dimensionless pressure adjacent to the vehicle, while all C_Q curves presented in Figure 5 monotonically and asymptotically approach a maximum value (C_{Qmax}). In order to maintain a low truck drag coefficient, it is desirable that the discharge air not be ejected with high velocities

perpendicular to the vehicle sides; therefore, the pressure within the hauler should be approximately equal to the exterior pressure adjacent to the vehicle ($C_{p_h} \simeq C_{p3}$). Values of $C_{Q_{max}}$ and the values of C_Q and A_3/A_1 corresponding to $C_{p_h} = 0.9\ C_{p3}$ are presented in Table 1 for each of the cases studied. These values of A_3/A_1 represent rough estimates that should be achieved to obtain relatively low discharge velocities perpendicular to the vehicle. More work needs to be done to refine these estimates. High A_3/A_1 values can be obtained by opening the sides (A_{3_s}) and/or the back (A_{3_b}) of the vehicle.

To illustrate the importance of using a diffuser to increase the flow rate through the vehicle, a comparison of values of C_Q at $C_{p_h} = 0.9\ C_{p3}$ in Table 1 for Cases 1 and 2 with $C_{p3} = -0.1$ and $K_3 = 0$ shows that the flow coefficient is increased 41% as C_{pd} is increased from 0 to 0.5.

To illustrate the concept of a backward flow model, comparing values of C_Q at $C_{p_h} = 0.9\ C_{p3}$ for Cases 2 and 3 with $C_{pd} = 0.5$ and $K_3 = 0$, about a 25% larger value of C_Q is obtained with $C_{p3} = -1$ (discharge in a low pressure region, e.g., near the top-front of the vehicle) and K_E as given by Figure 3 (NACA submerged entrances) as compared to $C_{p3} = -0.1$ (discharge near the rear) and $K_E = 0$ (inlet ram air). As shown by curves 3a and 3b in Figure 5, little difference in C_Q results by using different NACA submerged entrances. The mathematical model presented is valid only if no loss in total pressure occurs between the free-stream and the entrance. As indicated by Ahmed (16), a separation bubble occurs on the leeward side of a vehicle with yaw angles between 10^o and 30^o, with reattachment of the flow occurring downstream. Placement of the NACA inlets downstream of reattachment (using an internal backward flow model) would allow inflow at a wide variety of yaw angles, but could, with a fixed area design, result in poor natural ventilation at $V_\infty = 0$

(since parts of the upstream portions of the vehicle would not have openings). Also, a large boundary layer thickness at the entrance could result in poor diffuser performance.

Comparing values of C_Q at $C_{p_h} = 0.9\ C_{p3}$ for Cases 2 and 4 with $C_{p3} = -0.1$ and $C_{pd} = 0.5$, the values of C_Q are the same for $K_3 = 0$ (a well-formed discharge nozzle) and for the case with $K_3 = 1.5$ (a total pressure loss coefficient representative of that across an orifice plate which is typical of openings in some present-day haulers).

Comparing values of C_Q at $C_{p_h} = 0.9\ C_{p3}$ for Cases 4 and 5, with $C_{pd} = 0.5$, $K_3 = 1.5$ and $C_{po} = -0.1$, the value of C_Q is 10.9% larger for the case of inlet ram air with no entrance loss ($K_E = 0$) as compared to the case of using a NACA entrance with a peak RRR of 0.895. If sufficient ventilation can be achieved with ram air inlet, NACA submerged entrances should not be used. If NACA submerged entrances are used, they should be placed near the front and/or top of the vehicle; at yaw angles greater than 10^o, entrances on the leeward side of the vehicle would be in a region of separation and would probably experience outflow (see Ahmed (16)).

A comparison of the curves for Cases 4 and 6 with $C_{p3} = -0.1$, $C_{pd} = 0.5$, $K_3 = 1.5$ and $K_E = 0$, shows that the flow coefficient at $C_{p_h} = 0.9\ C_{p3}$ is decreased 10.5% when a flow distribution manifold with $C_M = 0.5$ is attached downstream of the diffuser (when $A_2/A_1 = 2$). As shown in the Appendix where manifold design is discussed, a discharge manifold with well-formed nozzles ($C_{dM} = 1$) and $A_M/A_2 = 1.4$, would have a manifold loss coefficient of 0.5. The use of a manifold is one way to achieve uniform flow distribution throughout the hauler.

EXPERIMENTAL SYSTEM AND PROCEDURE

In order to experimentally evaluate the drag and ventilation characteristics of tractor-trailer livestock haulers, five modified models and one unmodified model(i.e., representative of a current conventional or "typical" hauler) were constructed and evaluated at 0^{o} yaw angle in wind tunnels. Drag and ventilation measurements were made during these wind tunnel tests. Also, exterior static pressure distributions were obtained with an unmodified and a modified model, and limited studies in a full-scale unmodified vehicle were made.

All subscale models were experimentally evaluated in two wind tunnels; a description of each tunnel is presented in Table 2, and a sketch of each tunnel is presented in Figures 6 and 7. The draw-through tunnel was used for all drag and static pressure measurements, using tunnel velocities in the 20 to 29 m/s (66 to 95 ft/sec) range with $8.4 \times 10^{5} \leq R_e \leq 2.0 \times 10^{6}$, while the blow through tunnel with easy access and speed control was used for all flow visualization and ventilation studies using relatively low tunnel velocities (e.g., 0.1 to 1.5 m/s (0.4 to 4.5 ft/sec), with $3.8 \times 10^{3} \leq R_e \leq 1.0 \times 10^{5}$. The full-scale vehicle evaluation was made with a vehicle velocity of 22.4 m/s (73.3 ft/sec or 50 mph) with $R_e = 2.5 \times 10^{8}$.

Descriptions and sketches of each vehicle are presented in Table 3 and Figures 8 through 15. Model A is a subscale unmodified (i.e., typical) hauler. "Model"B is the full-scale unmodified tractor-trailer. Models C through E are subscale and modified for low drag at 0^{o} yaw (each have trailers with sharp-edged top longitudinal corners which would result in relatively

large drag at yaw) constructed to study the effectiveness of NACA submerged inlets and ram air inlets, manifold air distribution, and discharge design on the drag and ventilation characteristics of livestock haulers. Model F has rounded top longitudinal corners, and was designed to obtain desirable ventilation characteristics with a large value of A_3/A_{ts} and with rectangular shaped openings (the design was made after preliminary studies of Models A through E). The sides, roofs and tailgates of the trailers of models A, C, D, E, and F were contructed using transparent plastic to allow for flow visualization. Exterior static pressure taps were placed on Model G (an unmodified model) and Model H (a modified model without ram air or NACA submerged entrances) as shown in Figures 14 and 15.

Drag and static pressure measurements were obtained in the draw-through wind tunnel at zero yaw (exterior static pressure measurements were obtained at yaw angles of 0^o and 20^o) with models located approximately one vehicle length downstream from the leading edge of a ground plane. A sting balance and strain indicator with an output sensitivity of approximately 45 μ in./in. per N (200 μ in./in. per lb.) was used for drag measurements. Each model was free to move along the ground plane in the flow direction (the wheels were free to rotate) and was attached to the sting; each model was calibrated individually. Pressure taps attached to the rear of Model C were used to measure the interior hauler pressure. Pressure taps along the vertical and horizontal centerplanes of Model H were used to obtain exterior static pressures. Only the vertical centerplane of model G has pressure taps.

In order to obtain a quantitative assessment of the relative ventilation characteristics of each model, a solar cell was installed within each model at the upstream section of each hauler, and a light beam was aimed at the cell

through the transparent base region of the trailer from a location directly downstream of the hauler. Smoke was injected into the hauler and the voltage output of the cell, as recorded by a strip-chart recorder, changed from 0 to 1.5 volts as the smoke dissipated due to the influx of fresh air and the outflow of the smoke. A typical strip-chart recorder plot is presented in Figure 16, where t is the time required for the smoke in the hauler to dissipate enough so that ample light is incident upon the solar cell to produce a maximum voltage output. A dimensionless ventilation time parameter, $T = V_\infty t/L_t$, was obtained for each model. Also, a ventilation effectiveness parameter, N_V, representing the ratio of the theoretical ventilation time (via the mathematical model) to the actual ventilation time, (it can be shown that $N_V = WH_t/A_1 C_Q T$), was obtained for models for which mathematical values of C_Q existed.

The blow-through wind tunnel shown in Figure 7 was used for the flow visualization studies of the models. Flow velocities in the tunnel were maintained at a very low level (e.g., 0.1 to 1.5 m/s (0.3 to 4.5 ft/sec)) so as to improve visual perception of the smoke trails. A smoke generator was used which was constructed by placing a lighted cigar in a tube and passing air from a compressor over it and through a tube to selected positions on the model. The air flow patterns illuminated with smoke were photographed. In addition, tufts were placed near the openings on the side of the trailer to determine the direction of flow through the ventilation holes.

Full-scale tests were conducted on a conventional livestock trailer, hereafter referred to as "typical" or unmodified "Model" B, (gross weight limit of 27,273 kg (60,000 pounds) while it was pulled by a standard type tractor along the highway at 82 kph (51 mph). A smoke generator and tufts

mounted on long rods were used to indicate flow directions through the ventilation holes and within the hauler volume and an Alnor hand-held velometer was extended through the ventilation holes into the free stream flowing along the side of the trailer in order to determine the point where the flow reattaches. A hand-held thermoanemometer was used to measure flow velocities within the hauler volume.

RESULTS AND DISCUSSION

Drag Characteristics

Drag data for the models tested is included in Table 4. All values of C_D have an uncertainty of $\pm$ 7%, obtained using the Kline and McClintock (17) method with 20:1 odds. The Reynolds number range used was $1.1 \times 10^6 \leq Re \leq 2.0 \times 10^6$. The values of the drag coefficient (C_D) for each model did not change in this range.

Inspection of Table 4 reveals several important conclusions, among these are: 1) closing the gap and rounding the forebody of a tractor-trailer decreases the drag, 2) opening the sides of the trailer for ventilaton purposes results in a small increase of drag, and 3) opening the ram air or NACA inlets with open sides increases the drag. Discussion of each of these results follows.

Inspection of column I of Table 4 indicates that closing the gap and rounding the forebody reduces the vehicle drag. The major difference between Model A and the other models shown is the other models have closed gaps and rounded forebodies. Unmodified model A has a value of C_D of 0.91. In modified models C, D, E and F, C_D values range from 0.48 to 0.63. The values of C_D for model A compares favorably with the values obtained by Muirhead (5) for a similar model. The fact that model A does not have the side mirrors, horns or exhaust pipe accounts for an 8% lower value of C_D than obtained for Muirhead's model which had these devices. Values of C_D obtained for the modified models compared favorably with a value of C_D of 0.59 obtained by Muirhead for a vehicle with essentially similar modifications. Unvented

models D and F with C_D values of 0.53 and 0.48 respectively each have a more rounded forebody as compared to the forebody vertical corners of unvented models C and E with C_D values of 0.61 and 0.63 respectively. Marks (11) and Saltzman (7) have also indicated the importance of forebody rounding.

Comparisons of columns I and II of Table 4 indicate that the opening of the trailer sides for the purpose of ventilation results in a small increase in drag. Model F experienced a 12.5% increase. There were no significant changes in C_D values for models A and C. Apparently for the case with the inlets closed, air exits into the separation regions around the vehicle and the wake of the vehicle is not significantly altered when the ventilation occurs naturally. The large percent increase of C_D for model F could be attributed to a more streamlined shape for model F than for models C and D. Therefore, air discharge will have more effect on disrupting the external flow. Column III indicates the unexpected result that the drag is larger for model F if the tailgate is opened. The opening of the inlet also results in an increase in drag as shown by comparing columns IV and II. By comparing columns I and IV for models C, D, E, and F, it can be seen for model C that the C_D value increases by 27.9%, for model D increases 28.3%, for model E increases 30.2%, for model F increases 27.1%. The increase in C_D apparently is due to an increase in the size of the wake of each vehicle and occurs when ram air or NACA entrances exist and when air is forced through the discharge perpendicular to the vehicle as in model C, D, or F, or approximately parallel to the vehicle as in model E. The large values of C_D for model E can be ascribed to the large size of the discharge in relation to the size of the boundary layer at the location of the discharge.

It is interesting to note that for model C with the inlets closed, if the area ratio A_3/A_{ts} is increased by opening the tailgate from 0.078 to 0.172 (see columns II and III), the value of C_D does not change. For model F a change of A_3/A_{ts} from 0.153 to 0.250 increases the value of C_D. It should be noted that model C and F have different forebody radii. The rounding radius of model F is significantly larger than the radius of model C.

For the same changes of A_3/A_{ts} for models C and F with the inlets open, (see columns IV and V), the values of C_D decrease by 12.8% for model C and did not change for model F. The values of A_3/A_1 increase from 7.7 to 17.0 for model C and from 26.8 to 43.8 for model F. These data indicate that an optimum value of A_3/A_1 exists for minimum drag. A_3/A_1 is approximately 20 for minimum drag. Apparently the increase of A_3/A_1 reduces the discharge velocities perpendicular to the vehicle; however, a limit to this trend appears to exist. These conclusions were drawn using a limited amount of data. A more detailed inspection of these trends is needed.

Ventilation Characteristics

From consideration of the continuity equation, it is evident that for a given forward speed the inlet area and the velocity of air entering the trailer are dominant parameters associated with the ventilation time (as defined on page 16). The inlet area and air velocity are indirectly proportional to the ventilation time. Air enters the sides of the trailer when the sides are open and no ram air or NACA inlets exist. When ram air or NACA inlets do exist and

the sides are open, air enters through the inlets and the openings in the sides. It is therefore extremely difficult to determine the total area and/or the velocity of the air entering through these inlets.

Inspection of column I of Table 5 reveals that as A_3/A_{ts} increases from 0.078 for model C to 0.153 for model F the value of T decreases from 78 to 26. The increase of A_3 provides more area for the air to enter as well as exit from the trailer. There is insufficient data to determine the effect on T caused by closing the gap and rounding the forebody.

Comparison of data for model F in columns I and II suggests that the opening of the tailgate decreases the value of T whenever the ram air inlet is closed. The change in the value of T is small.

Inspection of columns I and III of Table 5 for model C shows that the value of T decreases from 78 to 36 when the ram air inlet is opened and A_3/A_{ts} is held constant. For model F the value of T does not change from a value of 26. Apparently the opening of ram air inlet causes air to cease entering or to enter some of the side ports more slowly. Column III also reveals that for model D with the upper chamber in the trailer open to the NACA submerged inlets and the lower chamber open to a ram air inlet, values of T were 46 and 43 respectively compared to model C which has a T value of 36. For data in column III the values of T for model D were lower compared to the value of T of 78 for model C in column I; this is a marked improvement. Therefore we conclude that the NACA inlets used in combination with the ram air inlet is effective but not as effective as the ram air inlet used alone. The degraded

performance of model D inlets could be caused by a relatively thick boundary layer at the entrance caused by low Reynolds number. Also, the lower chamber ram air inlet of model D had a curved diffuser which possibly effected its performance. It is of interest to note that the mathematical model did predict a 23% lower value of C_Q for the NACA submerged inlet of model D than for the ram air inlet of model F. Further inspection of column III for model F shows that increasing A_3/A_{ts} to 0.153 decreased the value of T to 26.

Column IV shows that for both models C and F the opening of the tailgate reduces the value of T. In the case of model C the value of T is reduced from 36 in column III for the tailgate closed to 27 for the tailgate open. The value of A_3/A_{ts} increases from 0.078 to 0.172. Values of T for model F decreased from 26 in column III to 21 in column IV, as the values of A_3/A_{ts} increased from 0.153 to 0.250.

Values of the ventilation effectiveness, N_v, varied from 11% to 55% for various models, and indicated the ratio of the theoretical time needed to fill the hauler with fresh air (assuming only fresh air comes in through the inlet and only used air exhausts through A_3) to the actual time required for the solar cell to indicate a maximum voltage output. Lower values of N_v can be caused by internal recirculation regions (mixing) or lower than theoretically predicted flow rates through the inlets due to, for example, Reynolds number effects. The highest value of N_v (N_v = 55%) occurred for Model F, the model with a diffused ram air inlet and a turning vane to distribute the fresh air, which appears to be a more effective way to obtain fresh air distribution as compared to the use of a manifold. The turning vane acts to distribute the

air directly downstream of the forward bulkhead, the region with most stagnation in the unmodified hauler. Also, Model F has openings on the truck sides with a larger length in the flow direction as compared to the other models. The geometry of the opening of the truck sides may be an important parameter influencing hauler ventilation and needs to be investigated further.

Flow Visualization:

The flow visualization studies revealed many interesting flow patterns in the hauling volume and along the sides of the vehicle. Only the typical hauler Model A, shown in Figure 8, and the modified Model C hauler with A_3/A_{ts} = 0.078, shown in Figure 10, have been used in flow visualization tests. Smoke flow studies for both 0^o and 20^o yaw angles were made. The flow inside Model A, a typical hauler, for 0^o yaw enters near the rearward portion of the sides of the trailer. The flow moves forward and exits near the forward end; relatively low velocities were observed near the forward end. Close inspection of Figure 17 indicates light air streaks near the aft end of the hauler and heavier smoke concentration near the center and forward end. The air, after exiting from the hauler, is swept along the sides of the trailer into the wake. At an approximately 20^o yaw angle (see Figure 18), air enters the hauler at most ventilation ports on the windward side and exits on the leeward side. A large wake exists on the leeward side. Figure 18 also shows a heavier concentration of smoke near the forward end of the hauler.

The flow for Model C with 0^o yaw enters through the ram air inlet, travels through the manifold and disperses into the upper and lower hauling chambers as shown in Figure 19. A heavier concentration of smoke is received

in the forward end of both chambers. The lower chamber tended to fill before the upper one, possibly indicating a non-optimum manifold design. Air exited through all ventilation ports and rolled into a vortex near the aft end of the trailer as shown in Figures 20 and 21. At yaw angles of approximately 20°, flow entered as before and the pressure within the hauling volume is sufficient to force air through all ventilation ports on both the windward and leeward sides of the trailer as shown in Figures 22 and 23. Figure 22 shows smoke exiting the windward side rolling over the top edge of the trailer and being intrained into the large wake on the leeward side.

Pressure Distribution:

Internal static pressure coefficients, C_{p_h}, measured as a function of A_3/A_1, were obtained for Model C at 0° yaw angle. A reasonably good agreement between the mathematical and experimental results is illustrated in Figure 24.

The external dimensionless static pressures, C_{pe}, measured at the points shown in Figures 14 and 15 of Models G and H were plotted versus position along the centerplanes of the models. Figures 25 and 26 depict the results for Model G at 0° and 20° yaw angles. These figures show that two stagnation points exist, one on the grill and the other on the forward bulkhead of the hauling volume. After stagnating on the grill, the flow accelerates over the cab creating a region of low pressure on the top of the cab. The flow then stagnates on the forward bulkhead of the hauler, creating a high pressure region on the upper portion of this surface. The flow separates over the top of the hauling volume because the upper edge is sharp. High velocities and low pressures are the result. The flow tends to reattach, the velocities

decrease, and the pressure coefficients increase, reaching a value of approximately -0.10 over the remaining portion of the roof. At a yaw angle of 20°, Figure 26, results are qualitatively similar to those at 0°yaw angle. However, the C_{pe} curves are slightly different since at yaw angles the body shape exposed to the flow is different. The most significant differences are the magnitude and size of the large negative C_{pe} region on the leading edge of the hauling volume and the magnitude of the roof top pressures for the trailer.

Figures 27, 28, 29, and 30 depict the results of the exterior pressure surveys of Model H. Figures 27 and 28 show values of C_{pe} along the longitudinal centerline at 0° and 20° yaw angles. Stagnation and values of C_{pe} equal to 1.0 were obtained on the surface facing the flow. The flow accelerates over the top surface creating peak negative values. These peak values are significantly different than for Model G since the forebody radii are significantly different and maximum velocities and values of C_{pe} depend on this parameter. In both cases, the values of C_{pe} approach approximately -0.10 as the flow decelerates on the upper surfaces of the two vehicles. The modest second negative peak for Model H curves is caused by a surface irregularity at the point where the forebody is joined to the hauling volume.

Figures 29 and 30, which depict values of C_{pe} obtained along the sides of Model H at 0° and 20° yaw angles, show the curves for the two yaw conditions to be qualitatively similar. Lower values of C_{pe} are obtained on the downwind side since a large separated region exists there. The negative values of C_{pe} on the leeward side increase as yaw angle increases.

Full Scale "Typical" Livestock Hauler Tests; "Model" B

In the over-the-road tests of a full-scale empty trailer (Figure 9) at 23 m/s (75 ft/sec or approximately 51 miles per hour) and 0^{o} yaw angle, flow was found to separate along the forward vertical edges of the trailer and reattach near the trailer's forward one-third section. The flow enters the trailer through the ventilation ports located in the mid one-third section of the trailer. Figure 31 shows the direction of flow in the rear of the trailer as indicated by a tuft mounted on a rod. There are several ports both forward and rearward of the mid one-third section where air is neither entering nor exiting. Some of the air that enters in the mid one-third section moves forward in the centerline section of the trailer. The remainder of the entering air moves aft along the sides and center section, is turned by the proximity of the solid, unvented tailgate, and either moves forward along the bottom of the trailer or exits through the ventilation ports to the rear. Air was found to enter the forward and exit the aft parts of some of the ports located in the rear one-third secton of the trailer. The maximum internal velocities at the centerline was approximately 0.1 V_{∞}. The forward one-third section of the trailer had the worst ventilation. The flow that moves forward from the mid section was turned by the proximity of the forward bulkhead and exits through the adjacent ventilation port (Figure 32). No perceptible air moved through about 20% of the ports in the forward one-third section. A load in the trailer would possibly block the forward flow and cause further deterioration of the ventilation of this section. In addition, the internal flow velocities were low in this region (approximately $0.03 < V/V_{\infty} < 0.06$). Figure 33 is a sketch of the hauler and the flow patterns in the hauling

volume.

In contrast to the typical full scale hauler where the air entered at the mid one third region, the air entered the rearward section of the sides of wind tunnel Model A and moved forward. A probable explanation for the difference is that at the higher Reynolds number of the flow over the full-scale trailer, the flow attaches further forward than it does for the model at low Reynolds number wind tunnel flow. In addition, a significant difference exists in the length of the side openings in the flow direction/truck side thickness ratio for the full-scale trailer and Model A, and the model and full scale tractors were of different types. The test of the full-scale trailer also revealed that at low speeds exhaust fumes accumulated in the forward one-third section, and the noise and vibration levels are very high at all speeds. These factors add to the stress to which the animals being transported are subjected.

CONCLUSIONS

A preliminary experimental wind tunnel investigation of the ventilation, flow visualization and drag characteristics of model livestock haulers, primarily at 0°yaw, has been made. In addition, a limited investigation of the flow visualization and ventilation characteristics was made of a full-scale livestock trailer at 0°yaw being pulled at 23 m/s (75 ft/sec or 51 mph)-nominal highway speeds. Wind tunnel models with several different configurations were tested. A typical unmodified model and vehicles modified for low drag and improved passive ventilation using ram air inlets, NACA submerged inlets, and without designed inlets were investigated. Air distribution through internal manifolds and with a vane, and discharge through orifice type openings and through well-formed nozzles were studied. Also, interior and exterior static pressure measurements were obtained. A mathematical model has been generated and used to provide guidance in selecting the configuration of the ventilation system for the modified models of this study, and can be used for the design of livestock haulers.

The conclusions that can be drawn from this investigation are:

1. The unmodified, or "typical", livestock hauler has a relatively high drag coefficient, and low velocity recirculation regions exist in the forward third portion of the hauler. Increasing the fraction of open area of the trailer sides of the unmodified model caused a moderate increase of vehicle drag.

2. Modification of a vehicle for low drag by using a rounded forebody

and enclosed gap (without ram air or NACA submerged inlets) has been shown to reduce the drag coefficient relative to an unmodified vehicle by 42%, and improves the ventilation by a factor of 2.5. Improved ventilation occurs as the fraction of open area of the trailer sides and/or tailgate (A_3/A_{ts}) increases, with a corresponding increase in the drag of a streamlined vehicle .

3. The addition of ram air inlets can be used to improve ventilation. Low velocity recirculation regions were observed in the forward third section of the unmodified hauler and modified (i.e., streamlined) vehicles without ram air inlets; these regions were eliminated by using ram air inlets. NACA submerged entrances do not provide ventilation as effective as ram air inlets, although the low Reynolds numbers of these tests may not provide proper conditions for evaluating the effectiveness of NACA submerged inlets for this kind of application.

4. A mathematical model has been developed which adequately predicts the ventilation characteristics of the hauler models with ram air and NACA submerged entrances.

5. Preliminary flow visualization studies were obtained and revealed a fairly good, i.e., qualitative, agreement between the flow in an unmodified subscale model and a typical full-scale livestock hauler trailer.

BIBLIOGRAPHY

1. "Recommended Practices for the Control of Bovine Respiratory Diseases in the Cow-Calf Herd." National Cattleman's Association and Association of Bovine Practitioners, [1975].

2. The Merck Veterinary Manual, 4th Edition, edited by O.H. Siegmund, Merck and Company, Inc. Rakway, New Jersey, 1973.

3. "A Guide to Environmental Research on Animals." Agricultural Board, National Research Council, National Academy of Sciences. Washington, D.C., 1971.

4. ASHRAE 1977 Fundamentals Handbook, Chapter 9, "Environmental Control for Animals and Plants - Physiological Considerations."

5. Muirhead, V.U. and Saltzman, E.J., "Reduction of Aerodynamic Drag and Fuel Consumption for Tractor-Trailer Vehicles." AIAA Journal of Energy, Vol. 3, No. 5, Sept-Oct, 1979. pp. 279-284.

6. Marks, C.H., Buckley, F.T. Jr., and Walston, W.H. Jr., "A Study of the Base Drag of Tractor-Trailer Trucks." ASME Journal of Fluids Engineering, Dec. 1978. pp. 443-448.

7. Saltzman, E.J. and Meyer, R.R. Jr., "Drag Reduction Obtained by Rounding Vertical Corners on a Box-Shaped Ground Vehicle." NASA TM X-56023, March, 1974.

8. Roshko, A. and Koenig, K., "Interaction Effects on the Drag of Bluff Bodies in Tandem." Aerodynamic Drag Mechanism of Bluff Bodies and Road Vehicles, General Motors Research Labs, Sept. 1976. pp. 253-286.

9. Mason, W.T. Jr. and Beebe, P.S., "The Drag Related Flow Field Characteristics of Trucks and Buses." Aerodynamic Drag Mechanism of Bluff Bodies and Road Vehicles, General Motors Research Labs, Sept. 1976. pp. 45-94.

10. Buckley, F.T. Jr. and Marks, C.H., "A Wind Tunnel Study of the Effect of Gap Flow and Gap Seals on the Aerodynamic Drag of Tractor-Trailer Trucks." ASME Journal of Fluids Engineering, Vol. 100, Dec. 1978. pp. 434-438.

11. Marks, C.H. and Buckley, F.T. Jr., "A Wind Tunnel Study of the Effect of Turning Vanes on the Aerodynamic Drag of Tractor-Trailer Trucks." ASME Journal of Fluids Engineering, Vol. 100, Dec. 1978. pp. 439-442.

12. Lissaman, P.B.S., "Research in Aerodynamic Drag Reduction of Trucks." Proceedings of the Second AIAA Symposium on Aerodynamics of Sports and Competition Automobiles, Los Angeles, California, May 11, 1974.

13. Kirsch, J.W., "Drag Reduction of Trucks with S^3 Air Vanes." Proceedings of the Second AIAA Symposium on Aerodynamics of Sports and Competition Automobiles, Los Angeles, California, May 11, 1974.

14. Muirhead, V.U., "An Investigation of Drag Reduction for Tractor-Trailer Vehicles." NASA CR 144877, Oct. 1978.

15. Mossman, E.A. and Randall, T.M., "An Experimental Investigation of the Design Variables of NACA Submerged Duct Entrances." NACA RM No. A7I30, Jan. 8, 1948.

16. Ahmed, S.R. and Hucho, W.H., "The Calculation of the Flow Field Past a Van with the Aid of a Panel Method." SAE Automotive Aerodynamics, Vol. 16, 1978, pp. 231-251.

17. Kline, S.J. and McClintock, F.A., "Describing Uncertainties in Single Sample Experiments." Mechanical Engineering, Jan. 1953. pp. 3-8.

18. Haerter, A.A., "Flow Distribution and Pressure Change Along Slotted or Branched Ducts." ASHRAE Journal, Jan. 1963. pp. 47-59.

19. Koestel, A. and Chia-Yung Young, "The Control of Air Stream from a Long Slot." ASHRAE Transaction No. 1429, 1951. pp. 407-418.

TABLE 1

Values of C_Q and A_3/A_1 at $C_{p_h} = 0.9\ C_{p3}$

Case	$C_{Q_{max}}$	C_Q at $C_{p_h} = 0.9\ C_{p3}$	A_3/A_1 at $C_{p_h} = 0.9\ C_{p3}$
1	1.049	1.044	10.44
2	1.483	1.476	14.76
3a	1.828	1.772	5.60
3b	1.888	1.833	5.80
4	1.483	1.476	23.35
5	1.338	1.331	21.04
6	1.327	1.321	20.88

Table 2

Wind Tunnel Description

Type	Draw-Through	Blow-Through
Test Section Dimensions	0.88 m (2.88 ft) high 1.18 m (3.87 ft) wide 1.52 m (5.00 ft) long	0.39 m (1.28 ft) high 0.56 m (1.84 ft) wide 0.97 m (3.17 ft) long
Test Section Maximum velocity	29 m/s (95 ft/sec) (at 40° setting)	21 m/s (68 ft/sec)
Contraction ratio	9.7 : 1	3.3 : 1
Upstream of Contraction	0.5 cm (0.2 in.) dia. 0.20 m (7-3/4 in.) long drinking straw followed by 4 - 0.16 cm (1/16 in.) mesh screens spaced 3.8 cm (1½ in.) apart	0.32 cm(1/8 in.) mesh honeycomb
Fan Type	Buffalo Arr. 9 Vaneaxial size 54C9	Joy Mfg. Axivane Series 1000
Motor horsepower/ speed	150 horsepower/1750 rpm	5 horsepower/860 rpm
Speed Control	Variable speed fluid drive unit	Variable pitch fan

TABLE 3A

Vehicle Dimensions

Vehicle	Description	Scale	A_3/A_{ts}	A_2/A_1	A_3/A_1	A_M/A_2
A	Unmodified single tier	1/25	0 to 0.086	-	-	-
B	Full scale vehicle	full	0.146	-	-	-
C	Diffused ram air inlet with distribution manifold, orifice discharge, two tier	1/25	0 to 0.172	-	0 to 7.7	2.1
D	Diffused ram air inlet with manifold for bottom tier, diffused NACA submerged entrance for top tier, orifice discharge	1/25	0 or 0.073	1.5(RAM) 1.5(NACA)	0 or 7.1(RAM) 0 or 4.6(NACA)	4.8 -
E	Diffused ram air inlet with nozzle discharge parallel to external flow, two tier, no manifold	1/18	0 or 0.082	3.5	0 or 5.1	-
F	Diffused ram air inlet with vane, orifice discharge, single tier, rounded horizontal corners	1/25	0 to 0.250	1.55	0 to 26.8	-
G	Unmodified model for exterior static pressure measurements	Same exterior dimensions as Model A (no ventilation features)				
H	Modified model for exterior static pressure measurements	Same exterior dimensions as Model D (no ventilation features)				

TABLE 3B

Vehicle Dimensions

Vehicle	L_V(m)	H_V/L_V	W/L_V	H_t/L_V	L_t/L_V	H_C/L_V	G/L_V
A	0.62	0.250	0.158	0.166	0.783	0.191	0.065
B	17.4	0.197	0.140	0.129	0.807	0.164	0.041
C	0.660	0.25	0.150	0.166	0.769		0*
D	0.692	0.250	0.147	0.163	0.785		0*
E	1.02	0.217	0.136	0.155	0.745		0*
F	0.689	0.244	0.138	0.167	0.708		0*

* G/L_V=0 because the gap was eliminated

TABLE 3C

Vehicle Dimensions

Vehicle	$A_{ts}(m^2)$ (both sides)	A_{3s}/A_{ts}	A_l/WH_t	A_{3b}/A_b	$A_p(cm^2)$
A	0.100	0 or 0.086	-	0	132.1
B (full size)	62.7	0.146	-	0	
C	0.111	0 or 0.078	0.104	0 or 1	149.5
D	0.123	0 or 0.073			156.4
Upper-NACA			0.170	0	
Lower-RAM			0.110	0	
E	0.242	0 or 0.082	0.190	0	282.9
F	0.117	0 or 0.153	0.061	0 or 1	149.6

TABLE 4

MODEL CONFIGURATIONS AND DRAG COEFFICIENTS AT 0^{o} YAW ANGLE

MODEL	I SIDES CLOSED INLETS CLOSED TAILGATE CLOSED $A_3/A_{ts} = 0$ C_D	II SIDES OPEN INLETS CLOSED TAILGATE CLOSED		III SIDES OPEN INLETS CLOSED TAILGATE OPEN		IV SIDES OPEN INLETS OPEN TAILGATE CLOSED			V SIDES OPEN INLETS OPEN TAILGATE OPEN		
		A_3/A_{ts}	C_D	A_3/A_{ts}	C_D	A_3/A_{ts}	A_3/A_1	C_D	A_3/A_{ts}	A_3/A_1	C_D
A	0.91	0.086	0.93								
C	0.61	0.078	0.62	0.172	0.62	0.078	7.7	0.78	0.172	17.0	0.68
UPPER NACA D LOWER RAM	0.53					0.073 0.073	4.6 7.1	0.68			
E	0.63					0.082	5.1	0.82			
F	0.48	0.153	0.54	0.250	0.60	0.153	26.8	0.61	0.250	43.8	0.61

TABLE 5

MODEL CONFIGURATION AND DIMENSIONLESS VENTILATION PARAMETERS

AT 0^{o} YAW

MODEL	I SIDES OPEN INLETS CLOSED TAILGATE CLOSED		II SIDES OPEN INLETS CLOSED TAILGATE OPEN		III SIDES OPEN INLET OPEN TAILGATE CLOSED						IV SIDES OPEN INLET OPEN TAILGATE OPEN					
	A_3/A_{ts}	T	A_3/A_{ts}	T	A_3/A_{ts}	A_3/A_1	T	C_Q	N_v	Case	A_3/A_{ts}	A_3/A_1	T	C_Q	N_v	Case
A	0.086	64														
C	0.078	78	0.172		0.078	7.7	36	1.28	21	6	0.172	7	27	1.32	27	6
D UPPER NACA					0.073	4.6	46	1.14	11	5						
D LOWER RAM					0.073	7.1	43	1.27	17	6						
E					0.082	5.1	14	1.43	26	4						
F	0.153	26	0.250	24	0.153	26.8	26	1.48	44		0.250	43.8	21	1.48	55	4

APPENDIX

Manifold Design

In manifold design, uniform distribution of the air is usually desired. Haerter (18) has shown that a constant area manifold with $L_M/D_{h2} < 200$ has a static pressure rise in the downstream direction caused by static pressure regain. Therefore, more flow is discharged from the downstream end of the manifold. At $L_M/D_{h2} = 200$, the frictional effects offset the basic pressure regain and a near constant manifold static pressure occurs, while a static pressure decrease occurs for $L_M/D_{h2} > 200$.

The uniformity of flow distribution for a manifold with non-constant static pressure is controlled by the area ratio of the manifold (A_M/A_2) and the geometry of the manifold discharge. Haerter also showed that for a constant area manifold, with $L_M/D_{h2} < 50$, A_M/A_2 must be < 0.735 to obtain a near uniform flow distribution when the manifold discharge is sharp-edged (the corresponding manifold pressure loss is as large as $2.5\,\rho V_2^2/2$), whereas A_M/A_2 may be as large as 1.05 if the manifold discharge is nozzle-shaped (and the corresponding manifold pressure loss approaches zero). If the A_M/A_2 ratios are more than three times larger than the value listed above, no flow will be discharged from the upstream portion of the manifold.

A manifold tapered to zero at the downstream end has a pressure drop along its length due to friction. Koestel (19) investigated the case of a tapered manifold with a slot discharge along the length of the manifold, assuming zero friction loss in the manifold. The pressure loss across the manifold and the angle of discharge from the manifold both decrease with increasing manifold area ratio as shown in Figure 34. To obtain uniform air

distribution in short manifolds ($L_M/Dh_2 < 200$), it appears that some taper is desirable; to obtain low pressure loss across the manifold, A_M/A_2 should be large, but cannot be too large or inflow could occur at parts of the manifold.

Using the static pressure vs. downstream position curves for constant area and tapered manifolds presented by Haerter, an estimate of the desirable taper for a constant pressure manifold was obtained and is presented in Figure 35. A hauler (Case 4) with a value of $A_M C_{dM}/A_2 \leq 1$ and $A_2/A_1 = 2$ would result in a large manifold pressure loss ($(P_2 - P_h)/\rho V_2^2/2) \geq 1$ and a corresponding decrease in the flow coefficient of $\geq 18\%$, while a value of $A_M C_{dM}/A_2 \sim 3$ could result in inflow into portions of the manifold. For hauler design, it is recommended to use Figure 35 to obtain the desirable taper and to choose a nozzle shape discharge geometry ($C_{dM} = 1$) with $A_M/A_2 \sim 2$. Current references for tapered manifolds need to be obtained and studied in more detail.

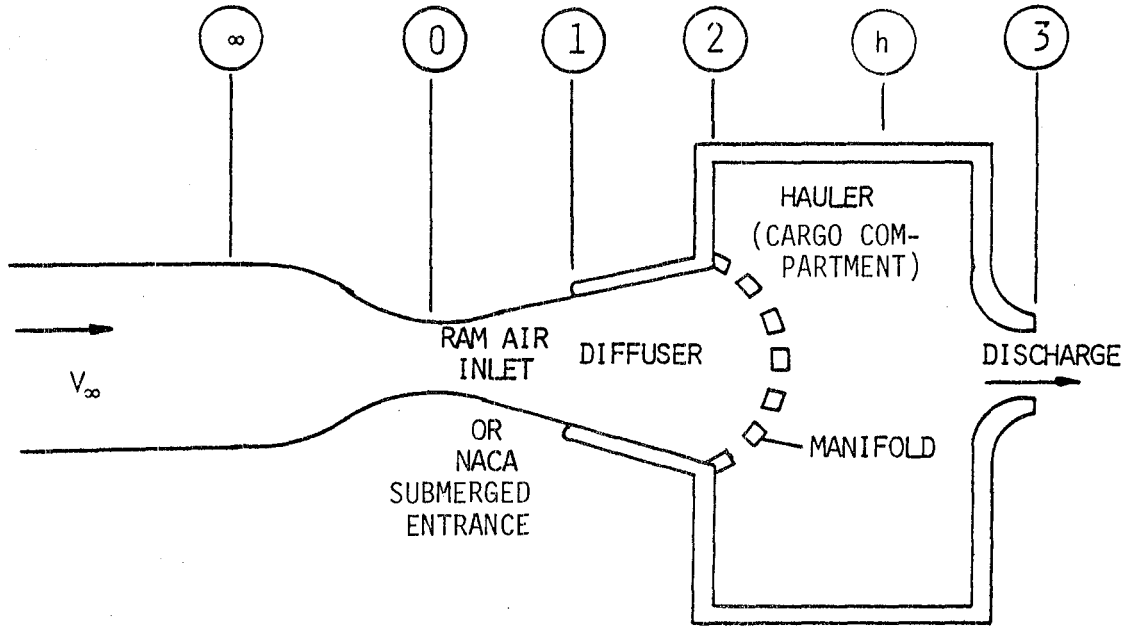

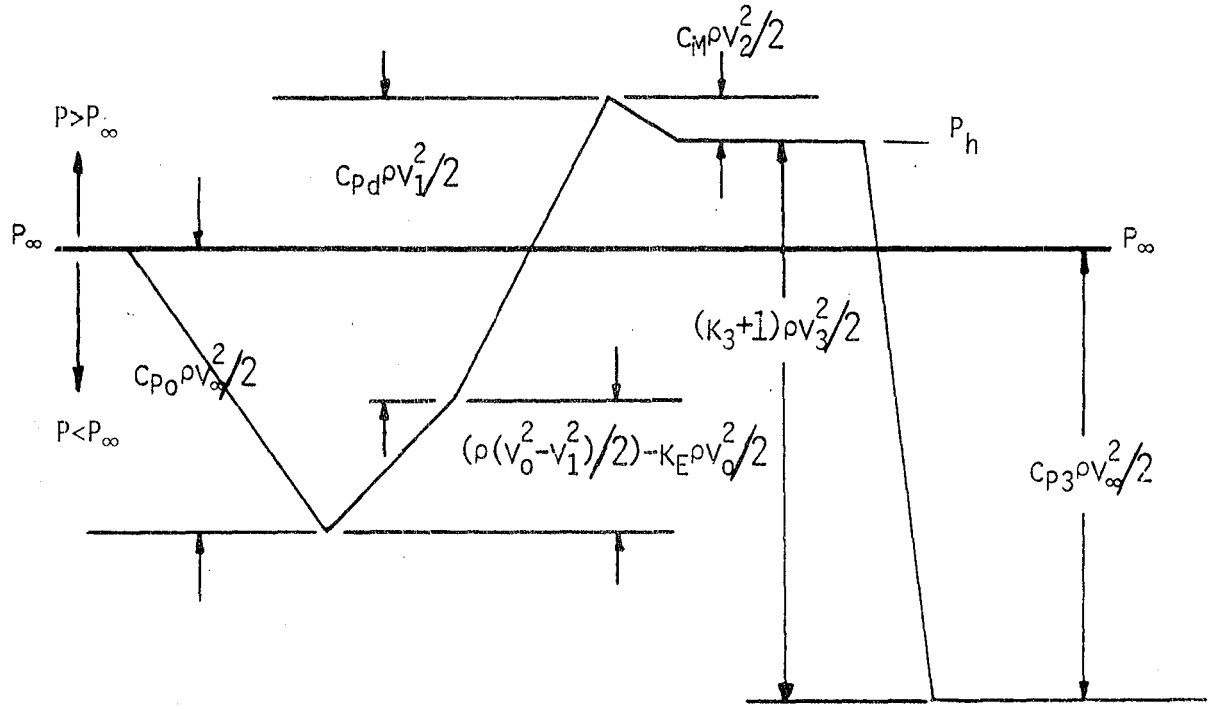

Figure 1

Model for Natural Ventilation Through a Moving Vehicle

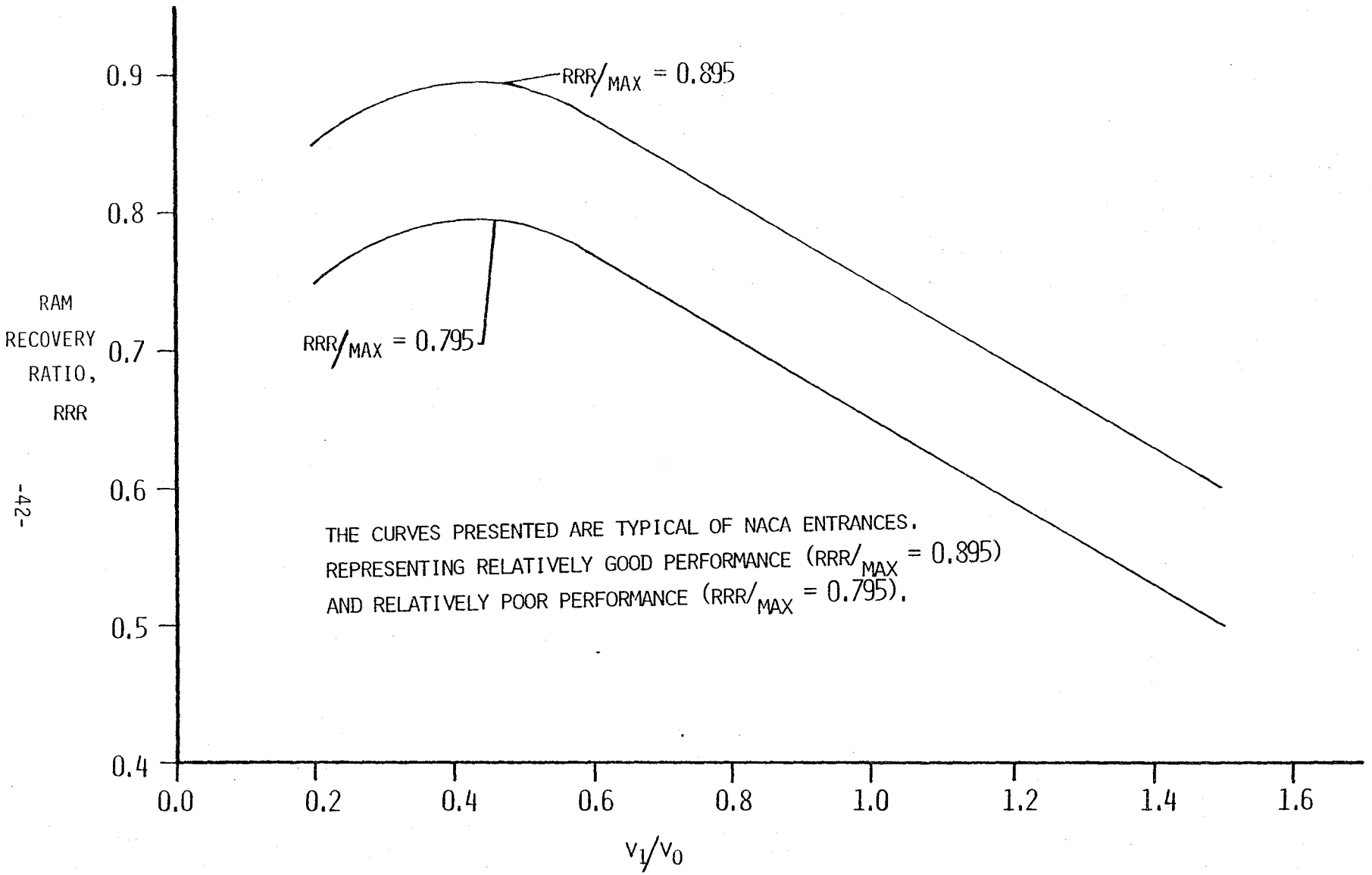

Figure 2

Ram Recovery Ratio vs. Velocity Ratio for Typical NACA Submerged Entrances

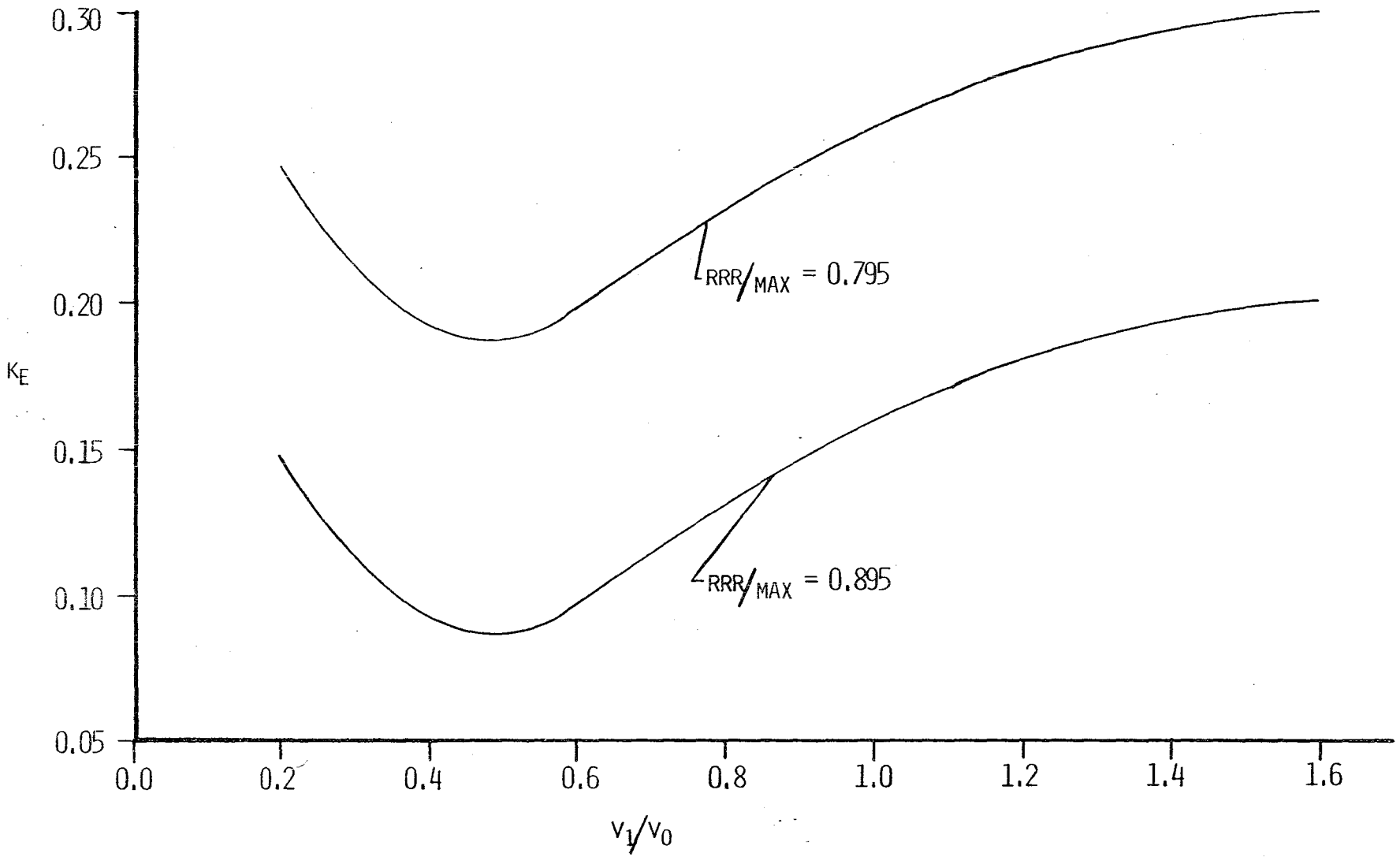

Figure 3

Total Pressure Loss Coefficient vs. Velocity Ratio for Typical NACA Submerged Entrances

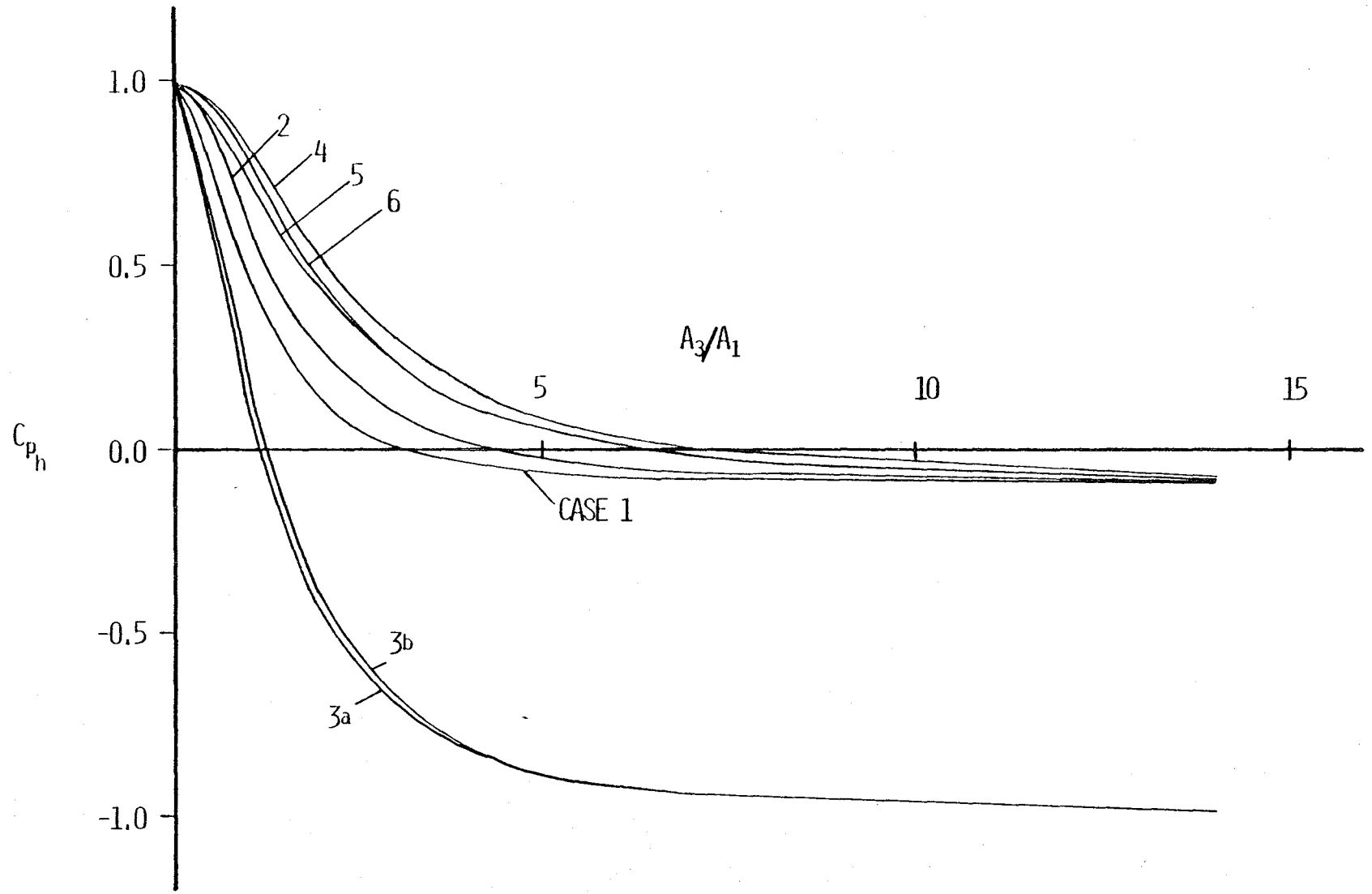

Figure 4

Hauler Pressure Coefficient vs. Area Ratio

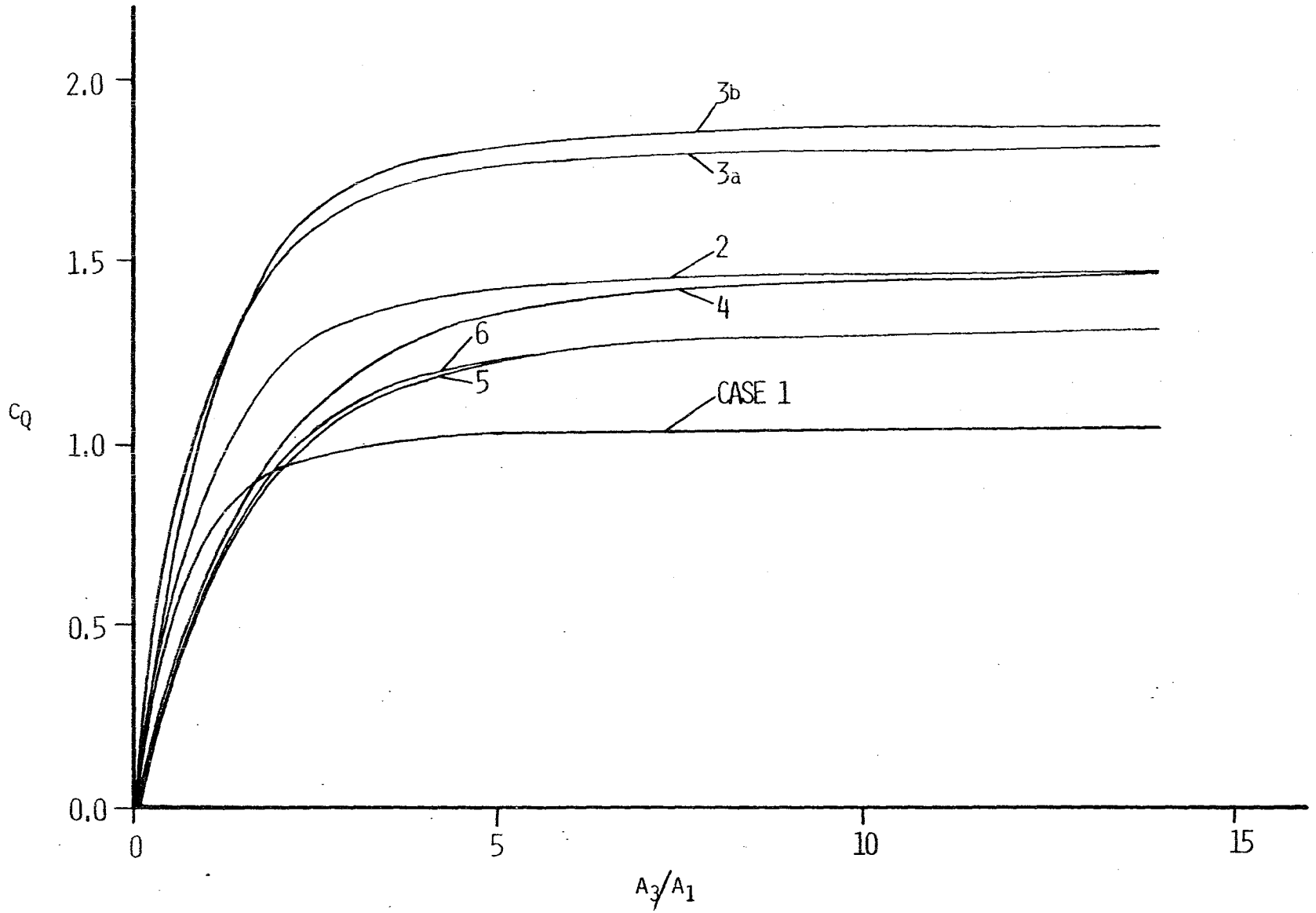

Figure 5

Hauler Flow Coefficient vs. Area Ratio

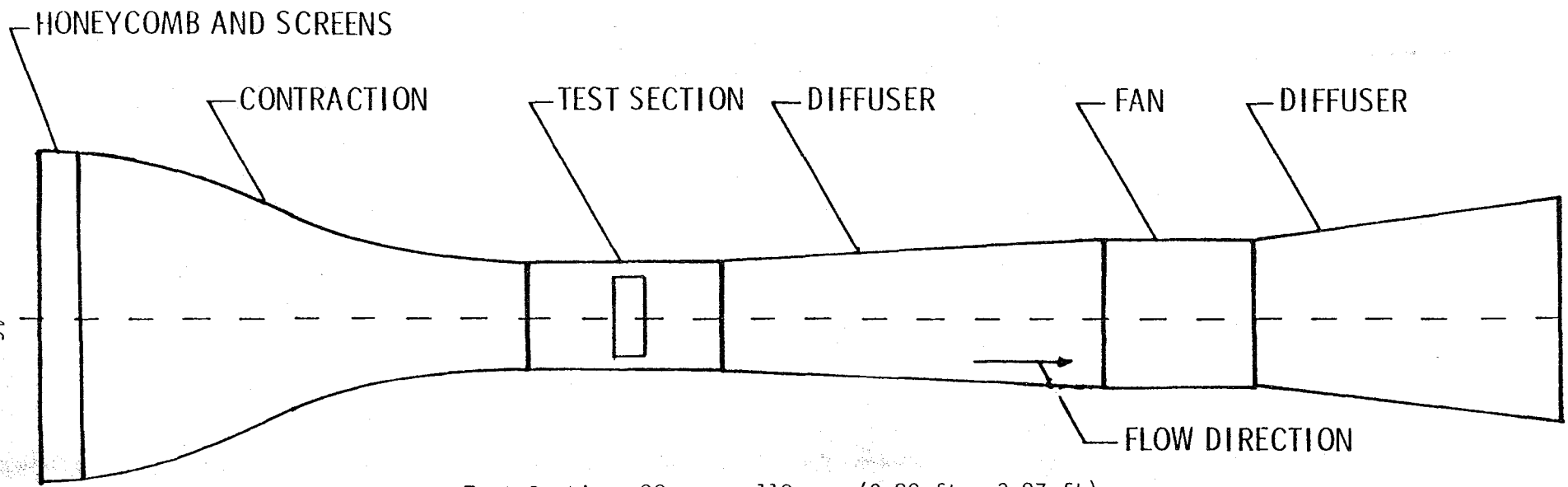

Test Section, 88 cm. x 118 cm. (2.88 ft x 3.87 ft)

Figure 6

Draw-Through Wind Tunnel

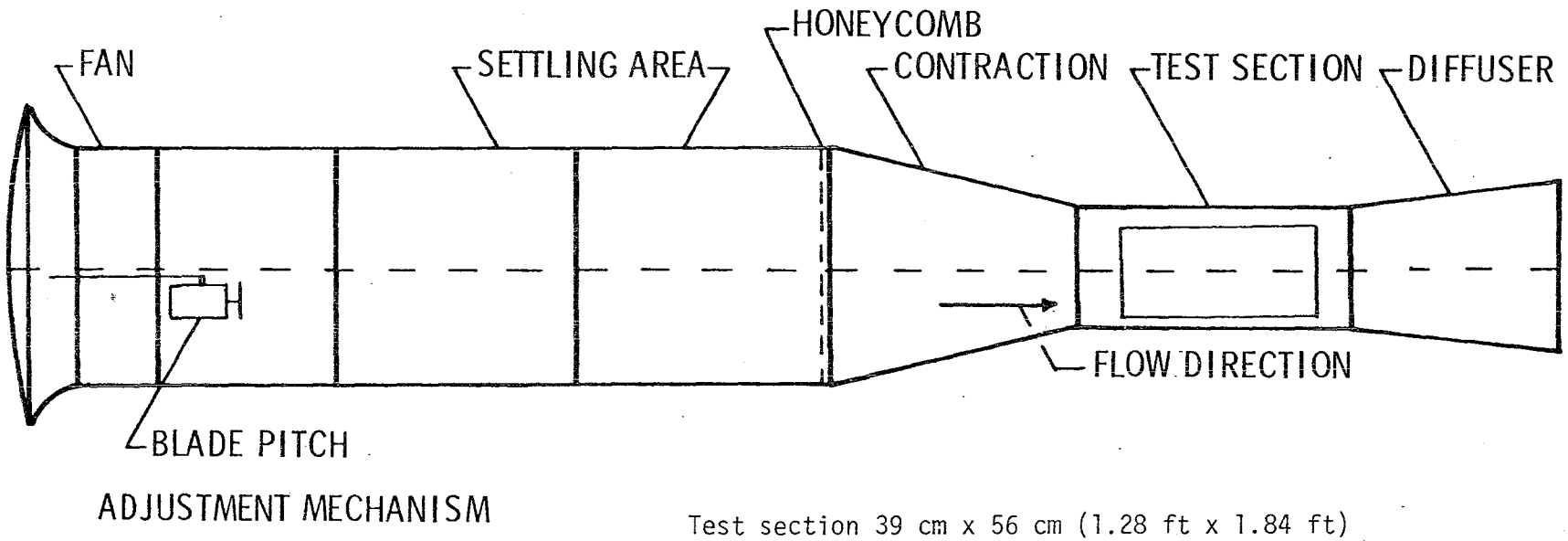

Test section 39 cm x 56 cm (1.28 ft x 1.84 ft)

Figure 7

Blow-Through Wind Tunnel

Top View

Side openings are uniformly distributed over trailer sides, and tailgate is unvented.

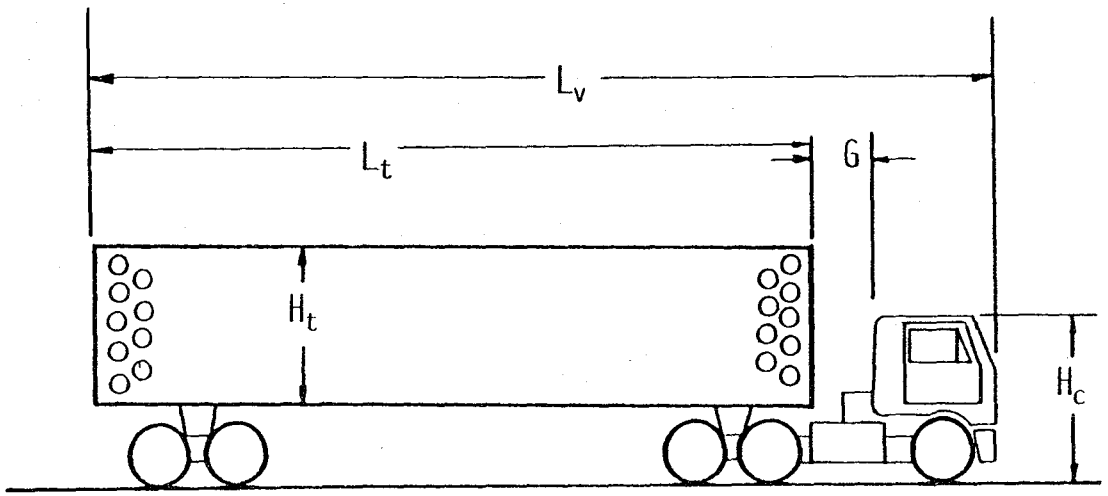

Side View

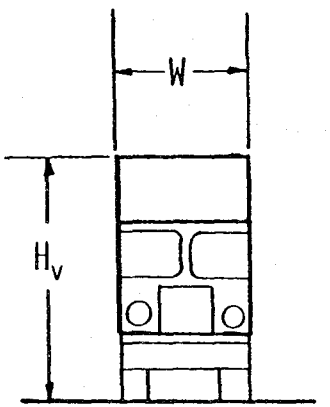

Front View

Figure 8

Model A, Typical Hauler

Top View

Side openings are uniformly distributed over trailer sides, and tailgate is unvented.

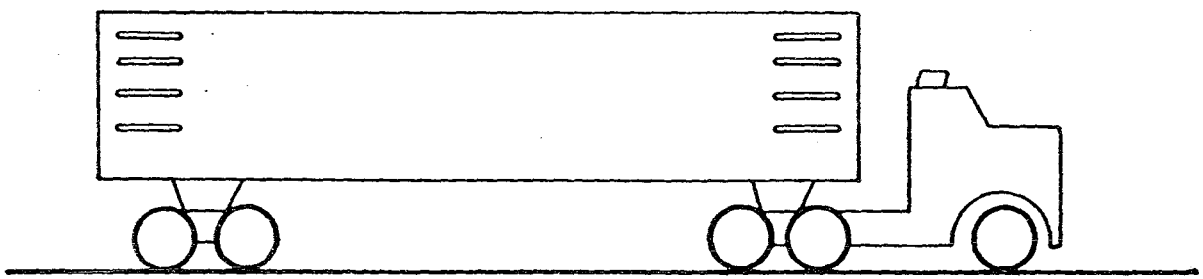

Side View

Figure 9

"Model" B

Full Scale Vehicle ("Typical")

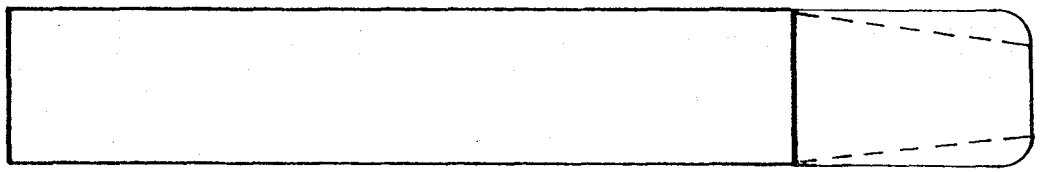

Top View

Side openings are uniformly distributed over trailer sides, and tailgate was vented or unvented.

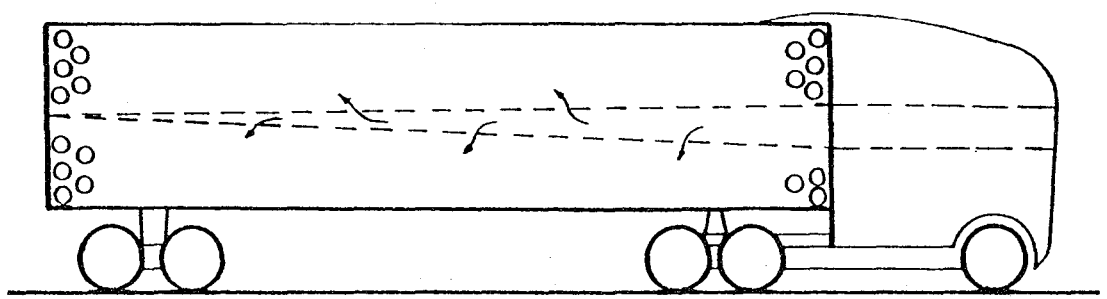

Side View

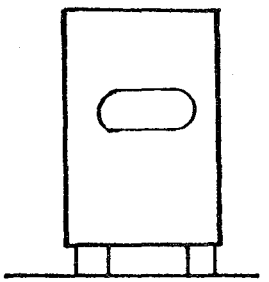

Front View

Figure 10

Model C

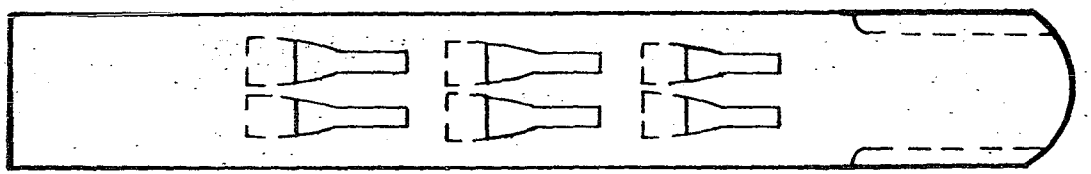

Top View

Side openings are uniformly distributed over trailer sides, and tailgate was unvented.

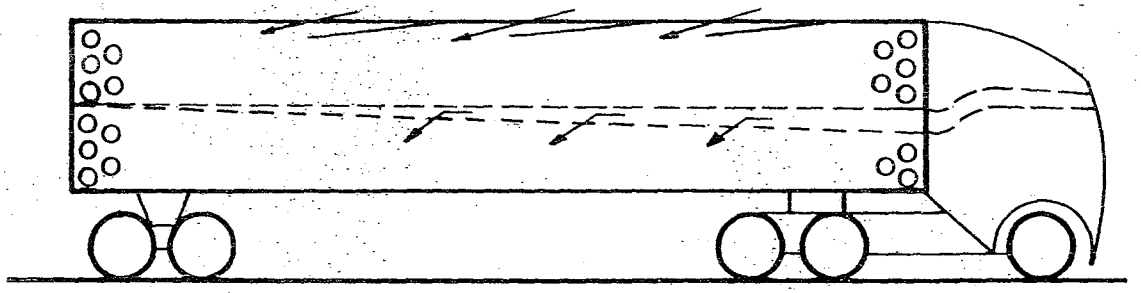

Side View

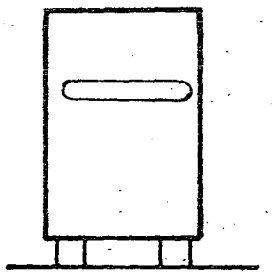

Front View

Figure 11A

Model D

NACA SUBMERGED ENTRANCE

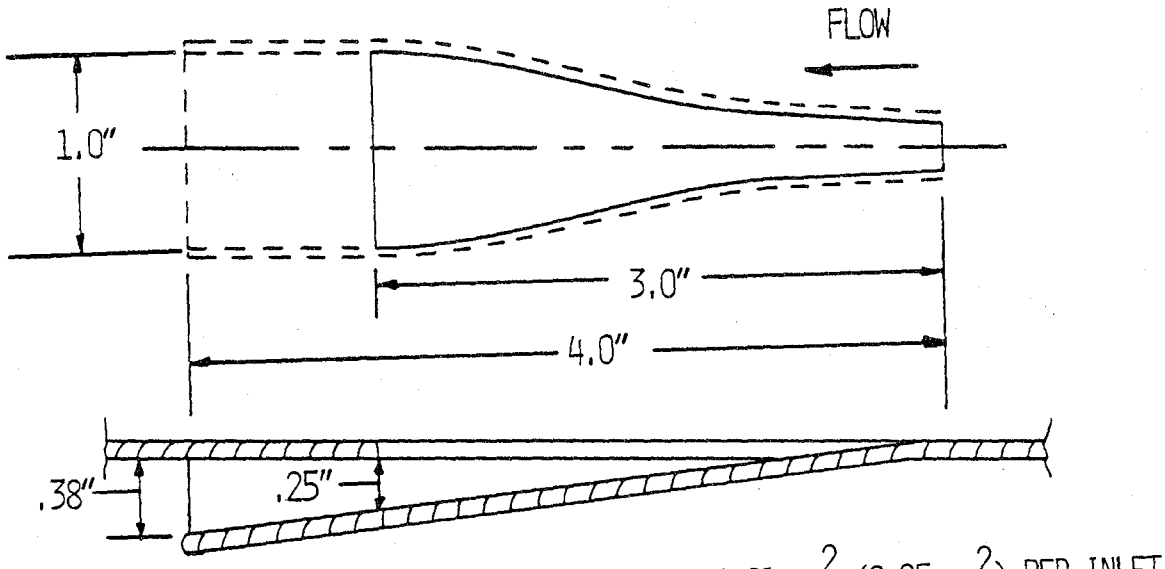

A_1 = 1.61 cm^2 (0.25 in^2) PER INLET

RAM AIR INLET AND DIFFUSER
SIDE VIEW

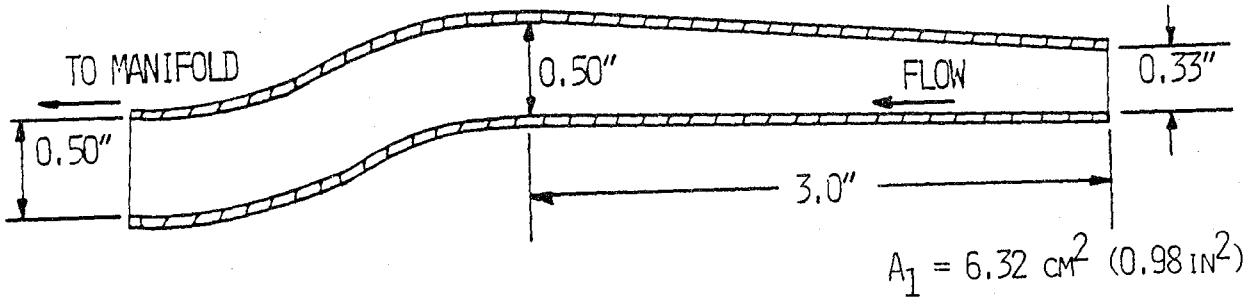

A_1 = 6.32 cm^2 (0.98 in^2)

Figure 11B

Inlets Used on Model D

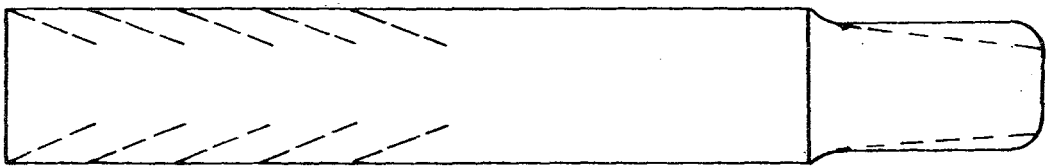

Top View

Tailgate was unvented.

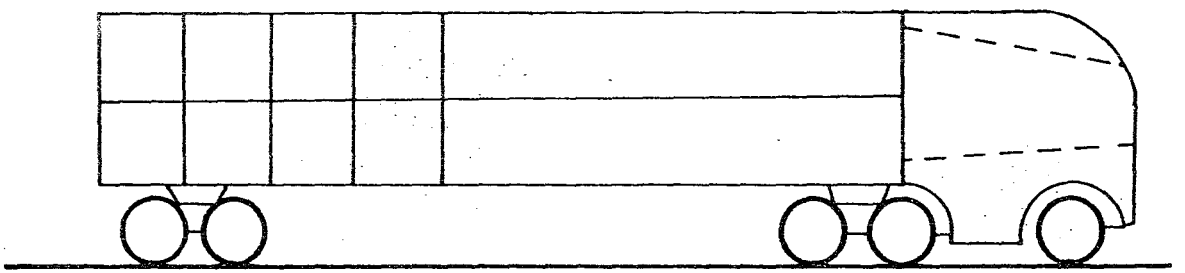

Side View

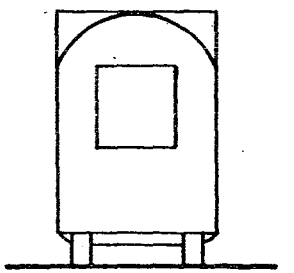

Front View

Figure 12

Model E

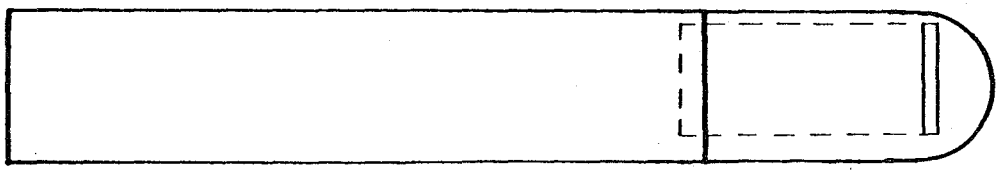

Top View

Side openings are uniformly distributed over trailer sides, and tailgate was vented or unvented.

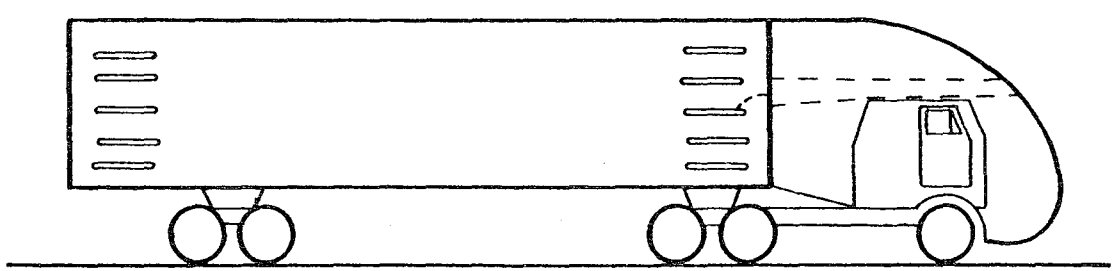

Side View

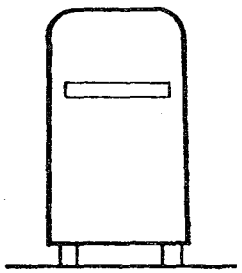

Front View

Figure 13
Model F

Top View

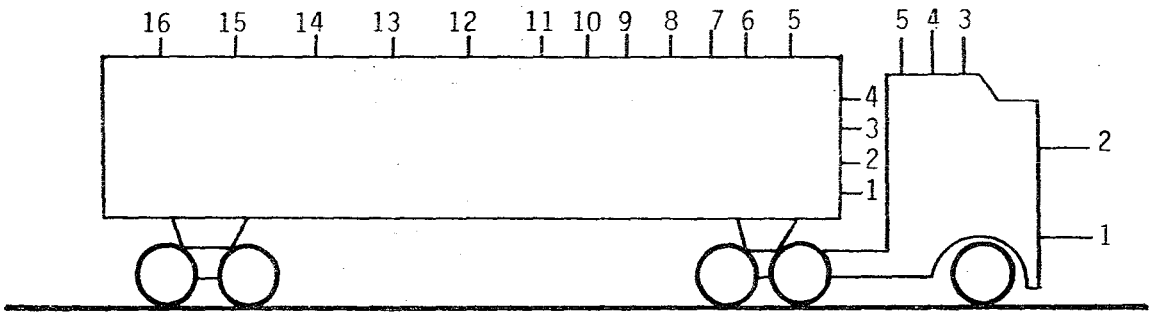

Side View

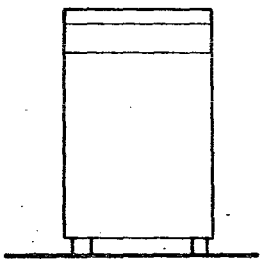

Front View

Figure 14

Model G

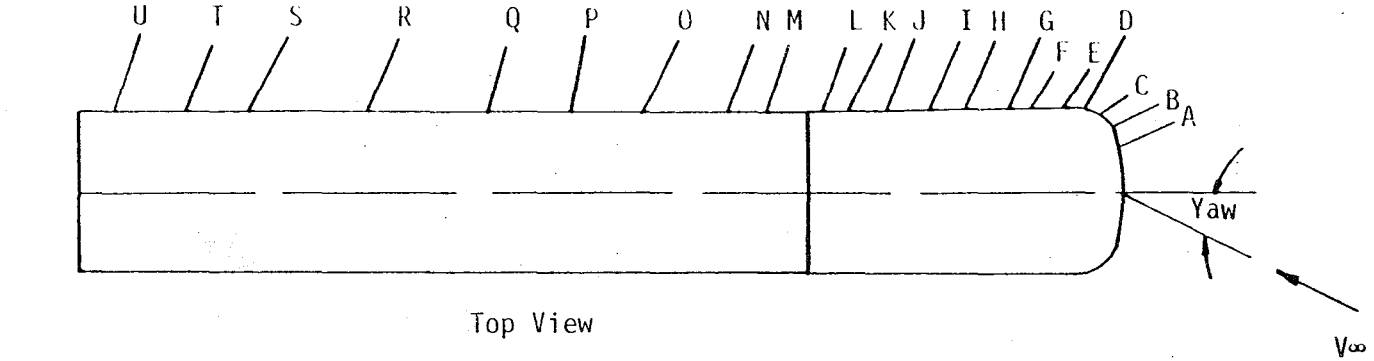

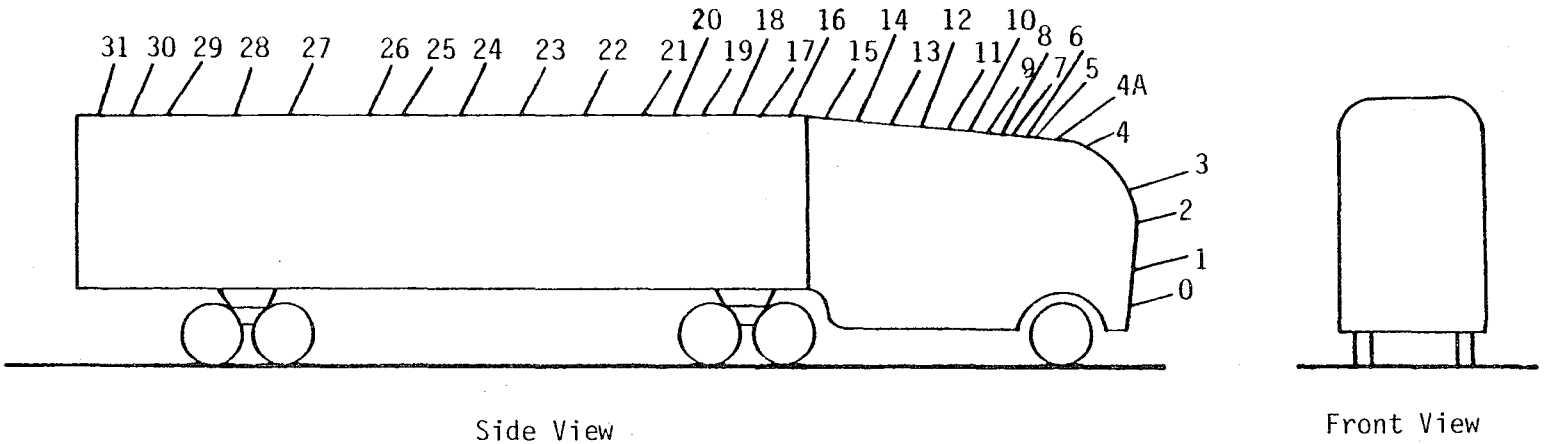

Figure 15

Model H

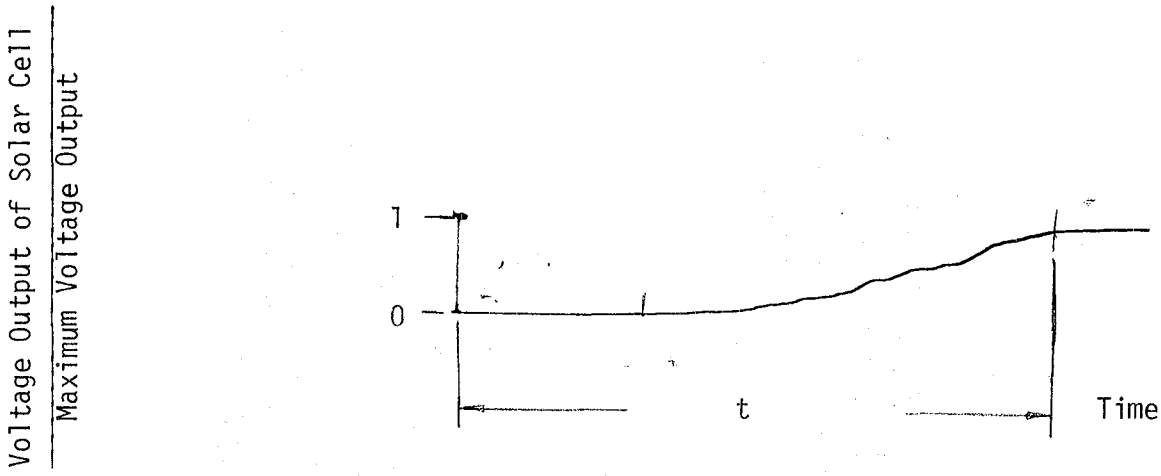

Figure 16
Solar Cell Voltage Output vs. Time-Ventilation Test

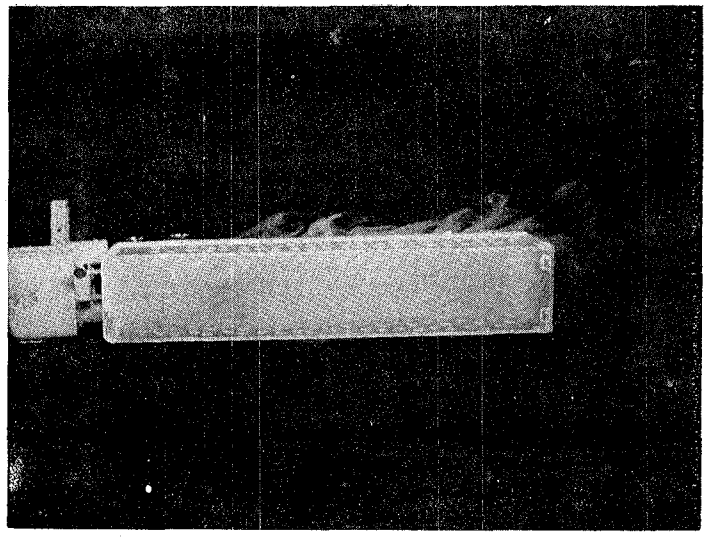

Figure 17
Top View of Model A, Typical Hauler, at 0^{o} Yaw

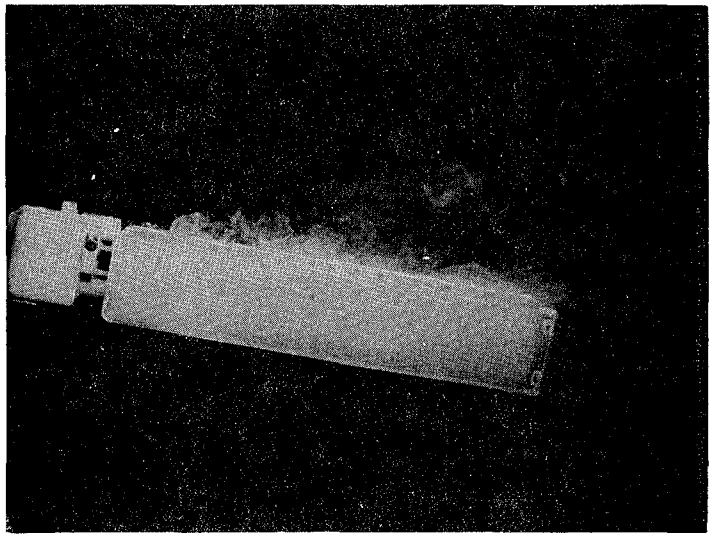

Figure 18

Top View of Model A, Typical Hauler, at 20^{o} Yaw

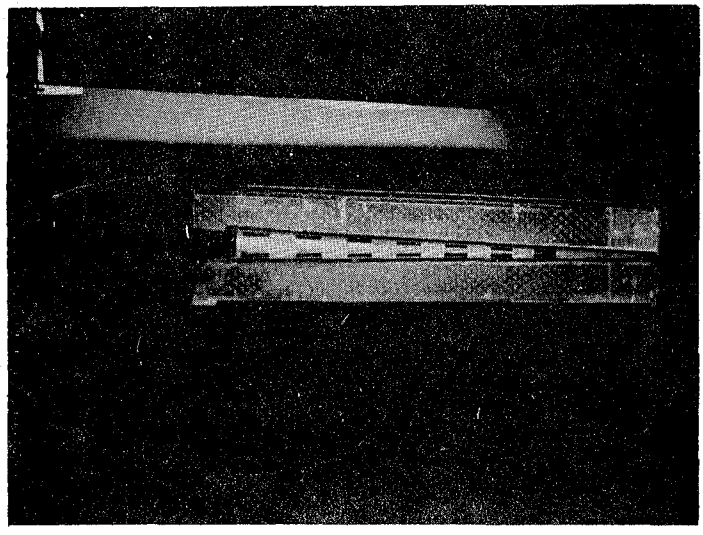

Figure 19

Side View of Model C, Modified with a Forward Facing Ram Air Inlet and Manifold, at 0^{o} Yaw

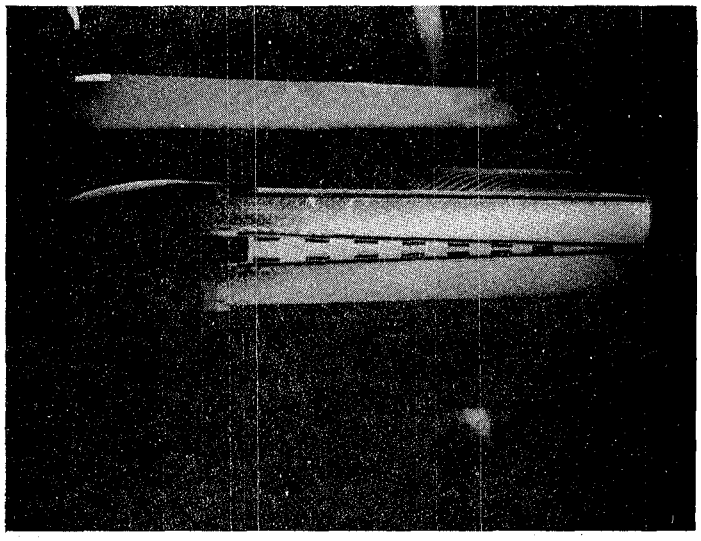

Figure 20
Side View of Model C, Modified with Forward Facing Ram Air Inlet and Manifold, at 0^{o} Yaw

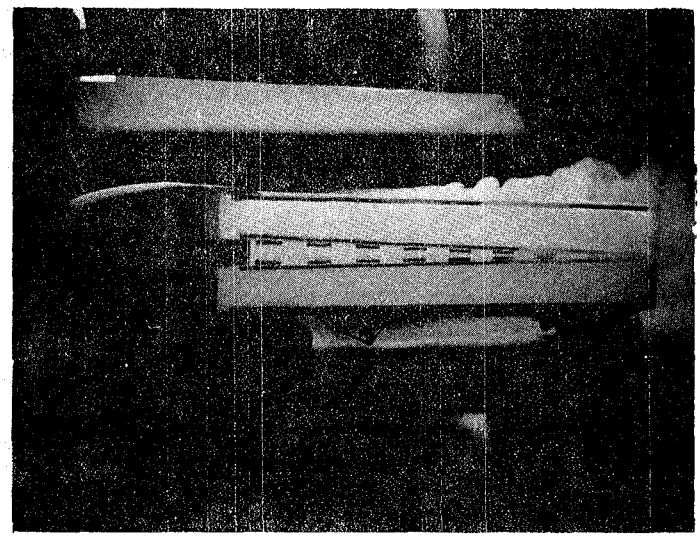

Figure 21
Side View of Model C, Modified with Forward Facing Ram Air Inlet and Manifold, at 0^{o} Yaw

Figure 22

Top View of Model C, Modified with Forward Facing Ram Air Inlet and Manifold, at 20^{o} Yaw

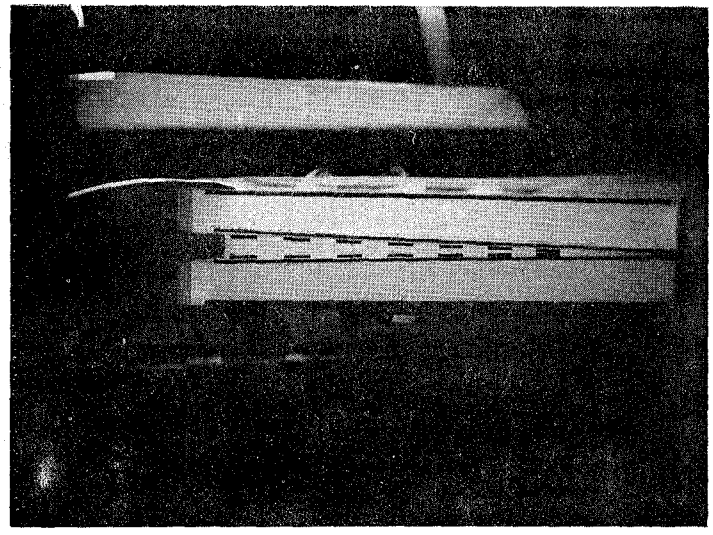

Figure 23

Windward Side View of Model C, Modified with a Forward Facing Ram Air Inlet and Manifold, at 20^{o} Yaw

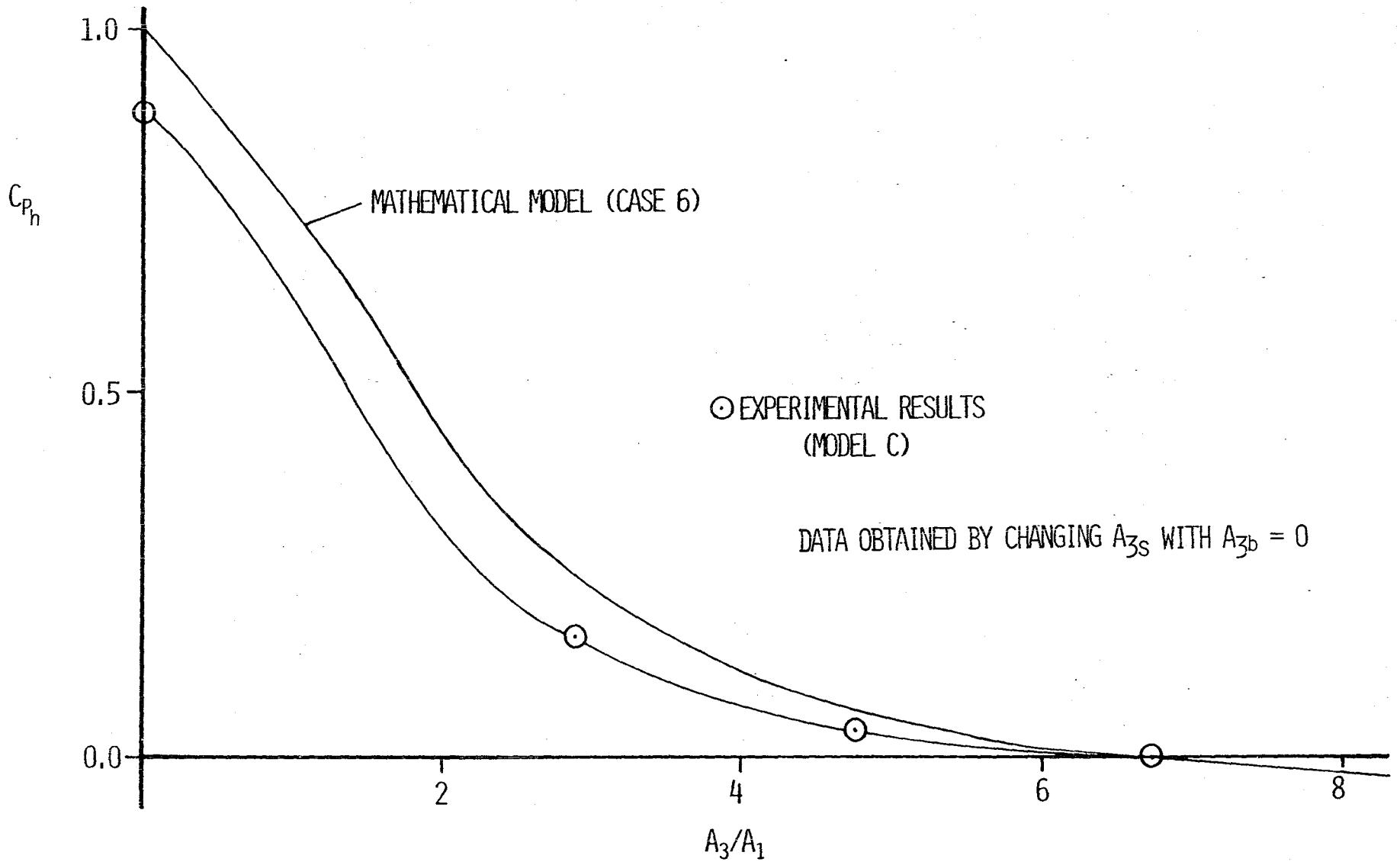

Figure 24

Internal Static Pressure Coefficient vs. Area Ratio

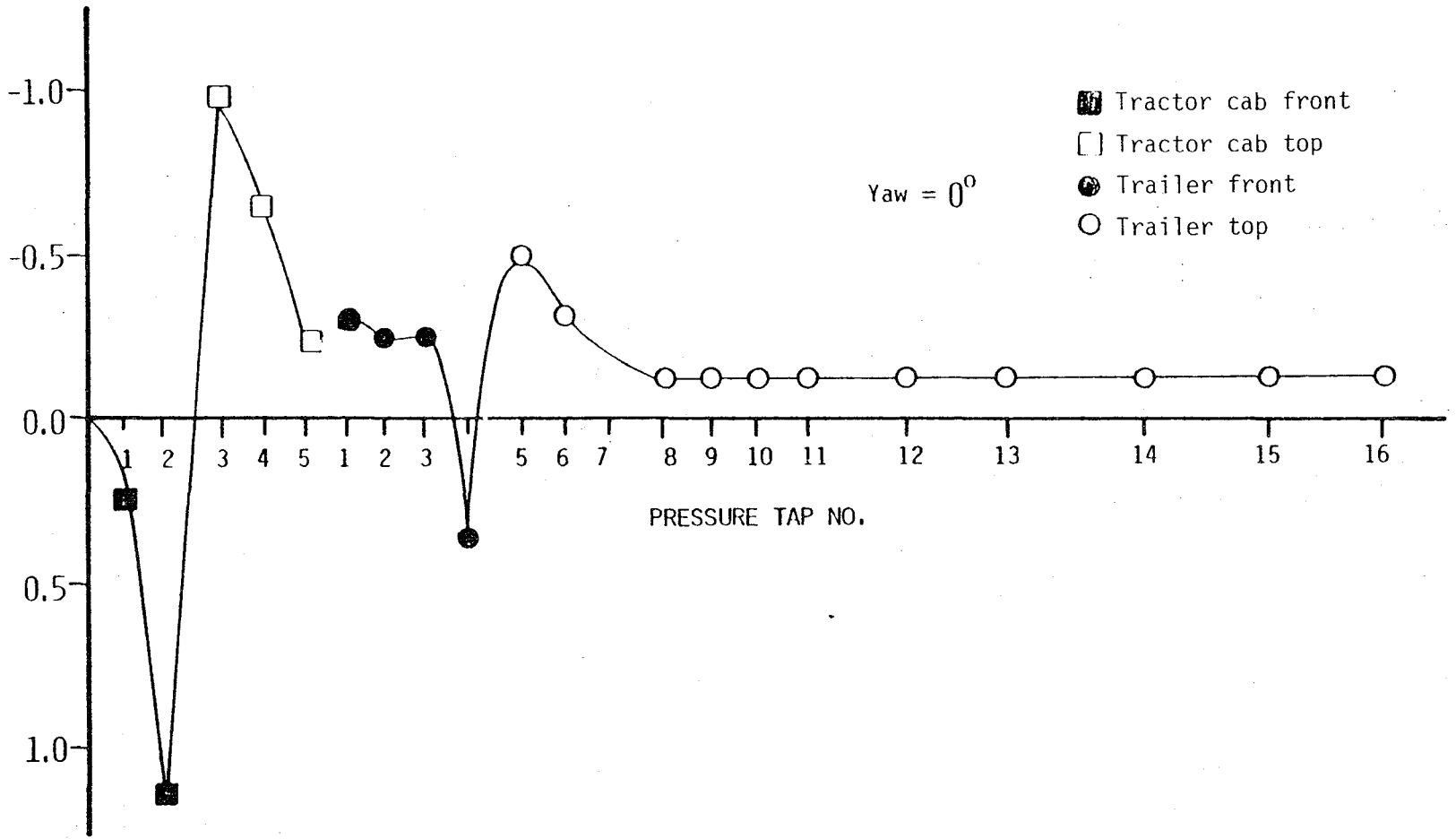

Figure 25

C_{pe} vs. Position along Vertical Centerplane of Model G at 0^{o} Yaw

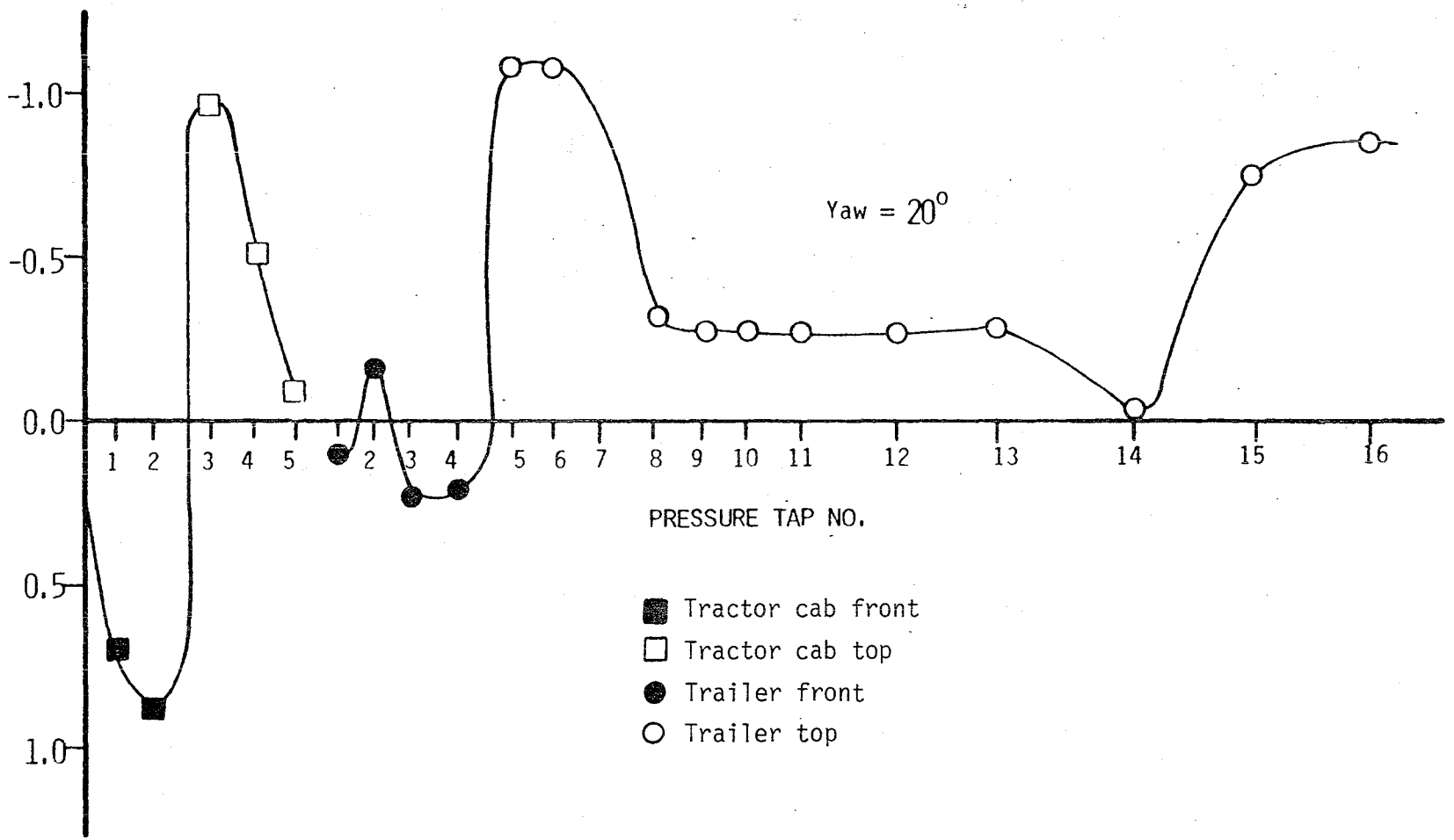

Figure 26

C_{pe} vs. Position alongVertical Centerplane of Model G at 20° Yaw

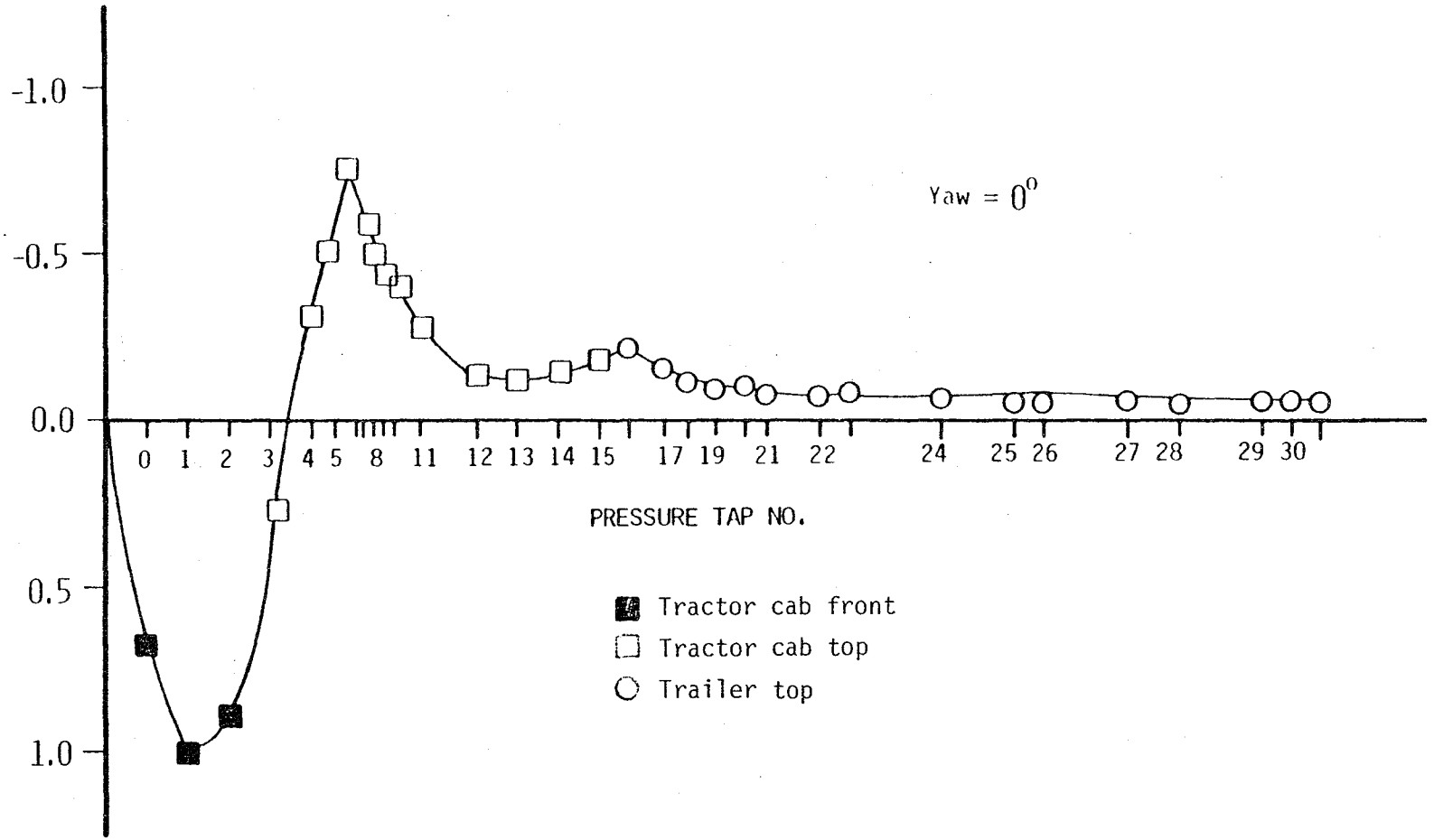

Figure 27

C_{pe} vs. Position along Vertical Centerplane of Model H at 0^o Yaw

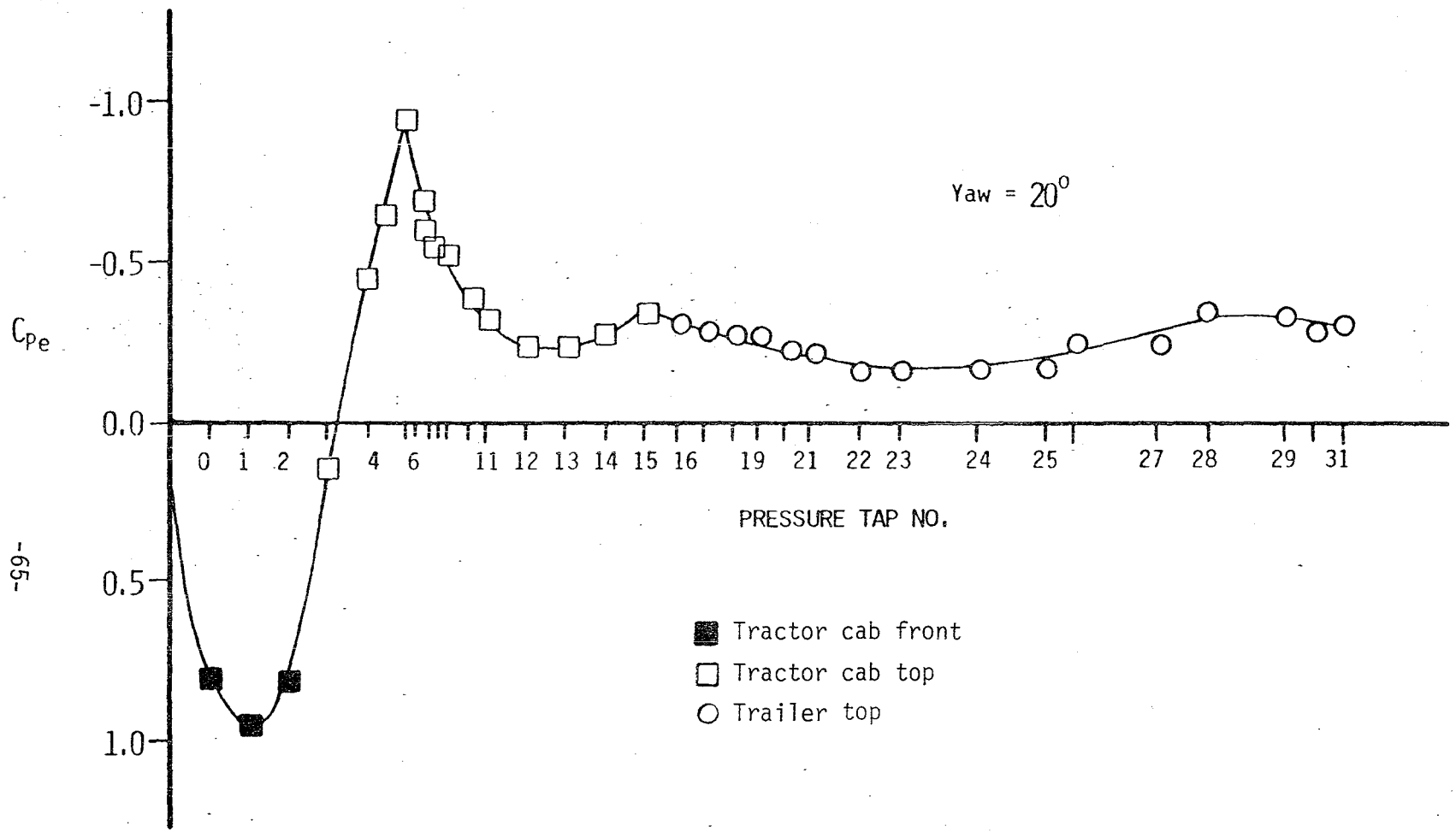

Figure 28

C_{pe} vs. Position along Vertical Centerplane of Model H at 20° Yaw

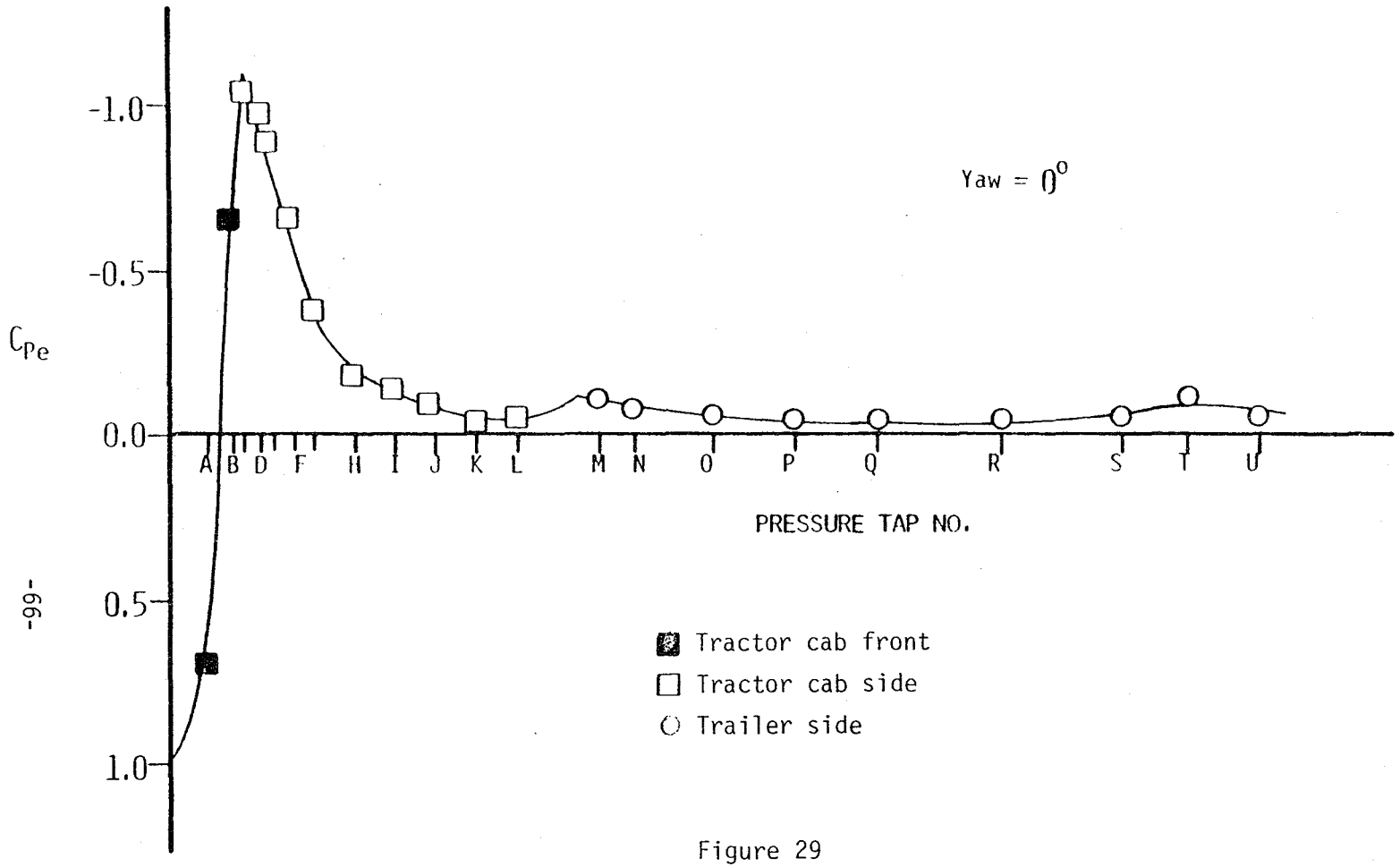

Figure 29

C_{pe} vs. Position along Horizontal Centerplane of Model H at 0^o Yaw

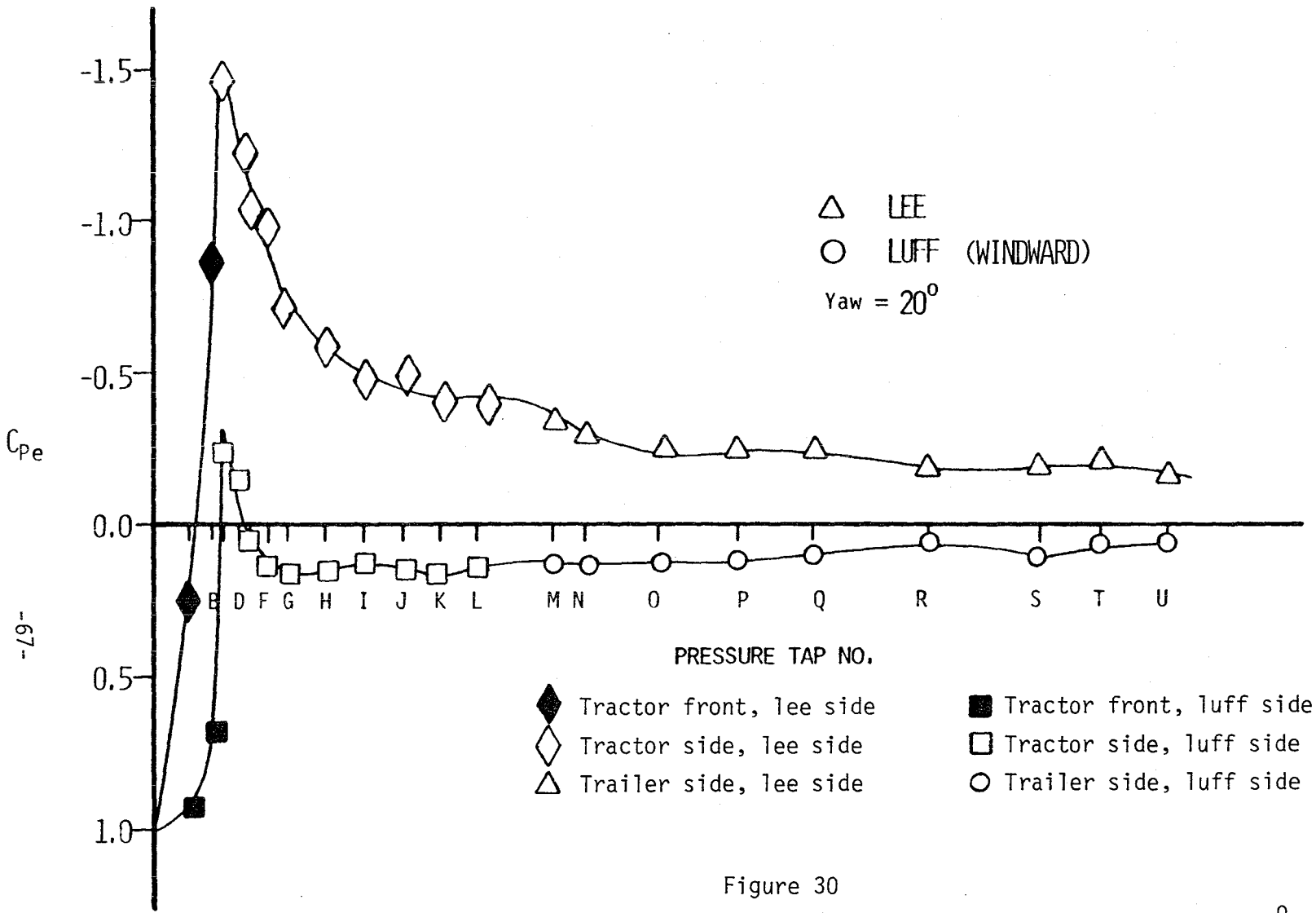

Figure 30

C_{pe} vs. Position along Horizontal Centerplane of Model H at 20° Yaw

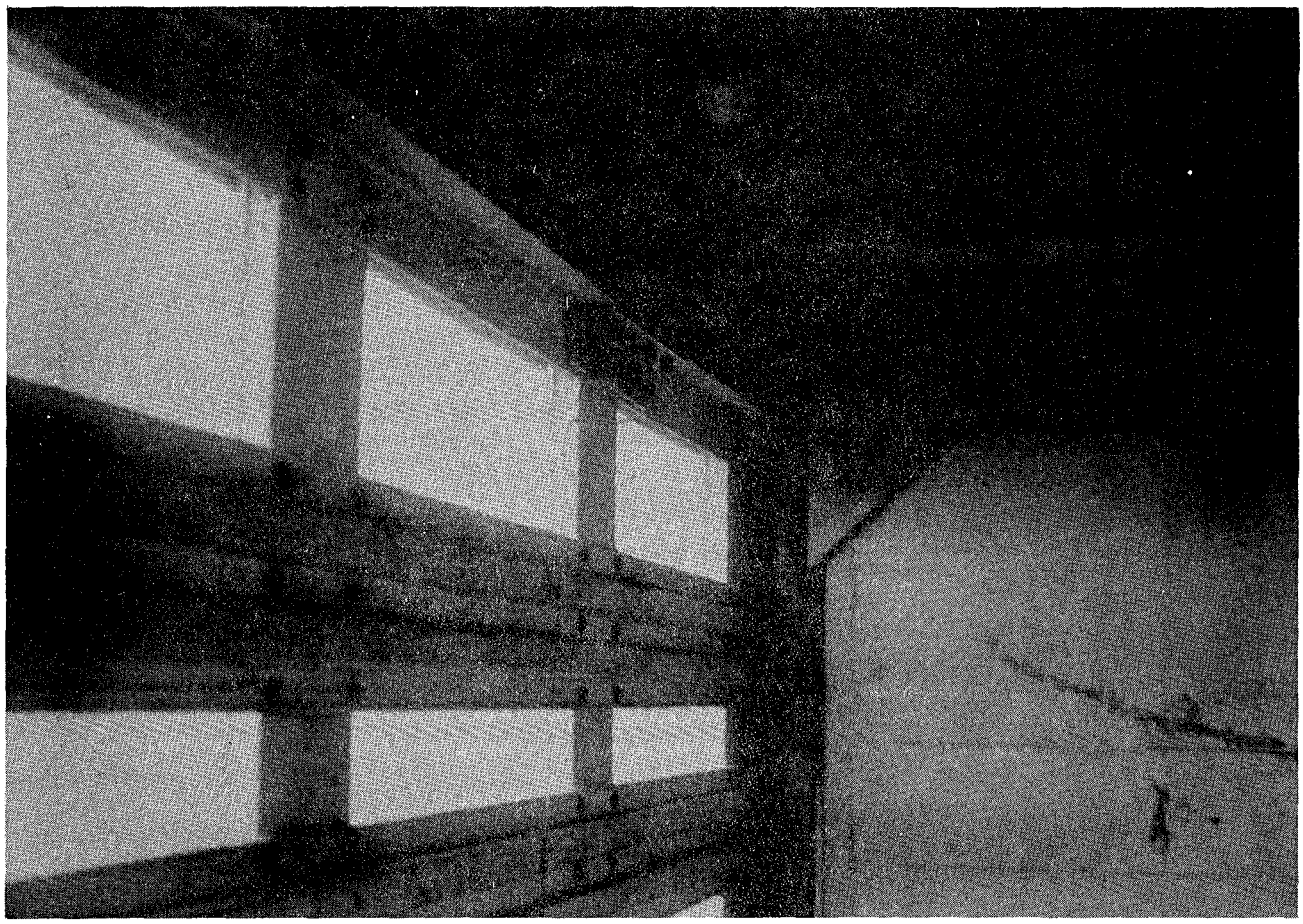

FIGURE 31

INWARD FLOW, INDICATED BY THE TUFT, THROUGH VENTILATION SLOTS NEAR REARWARD END OF A FULL-SCALE TRAILER

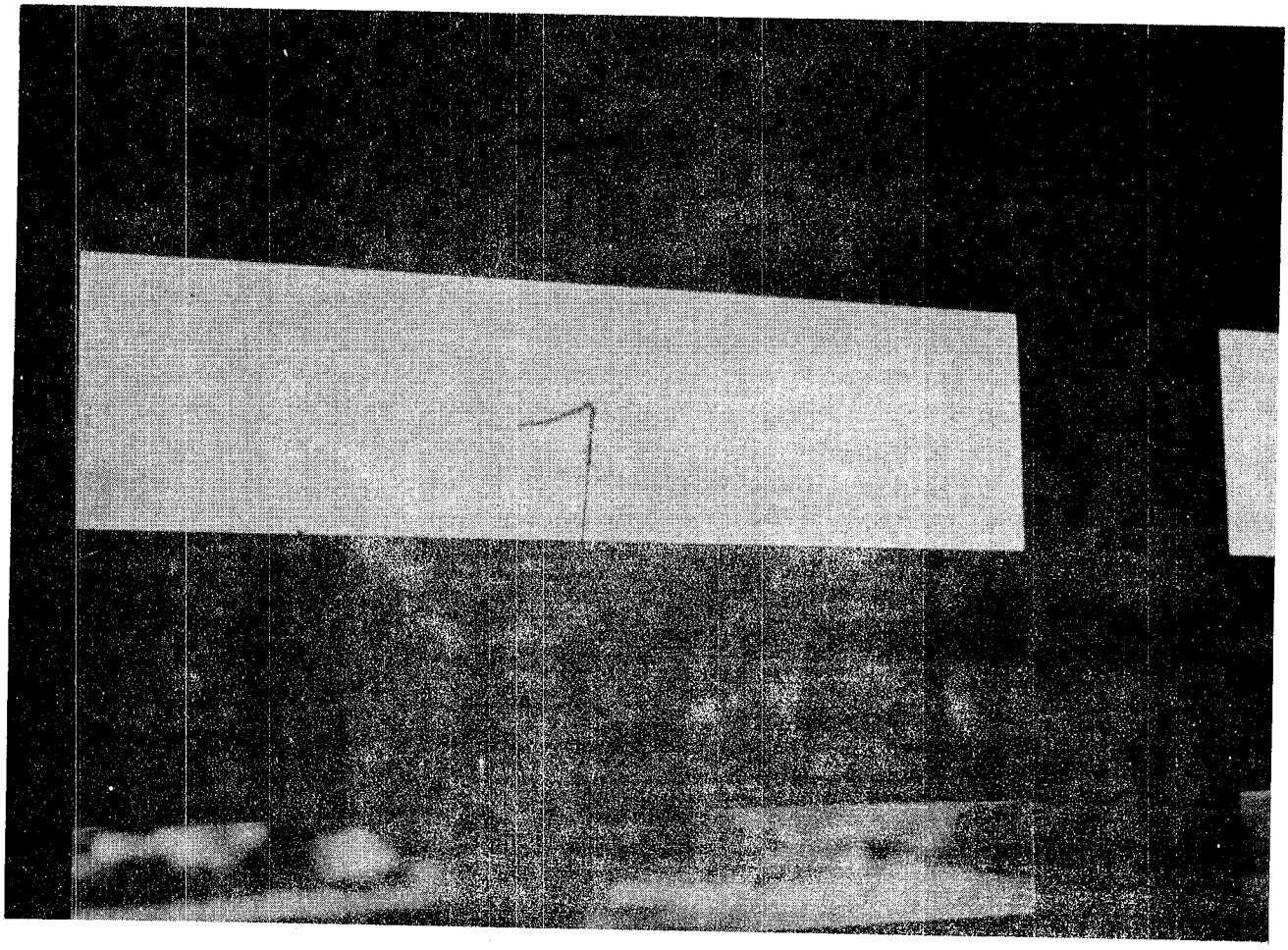

FIGURE 32

OUTWARD FLOW, INDICATED BY THE TUFT, THROUGH VENTILATION SLOT NEAR FORWARD END OF A FULL SCALE TRAILER

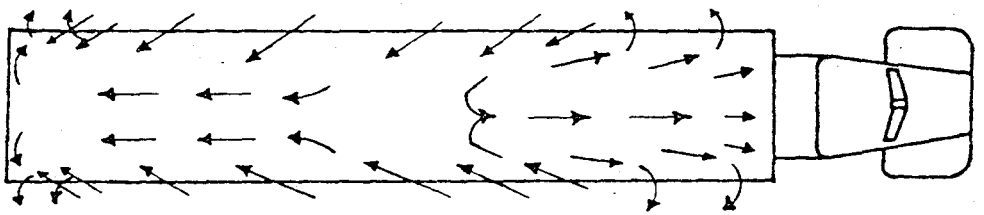

Top View

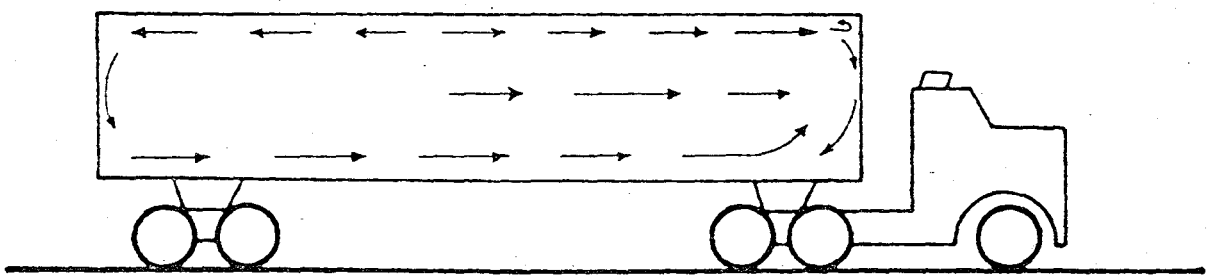

Side View

Figure 33

Flow Patterns in Hauling Volume of "Typical"
Full-scale Livestock Trailer, Yaw = 0^{o}

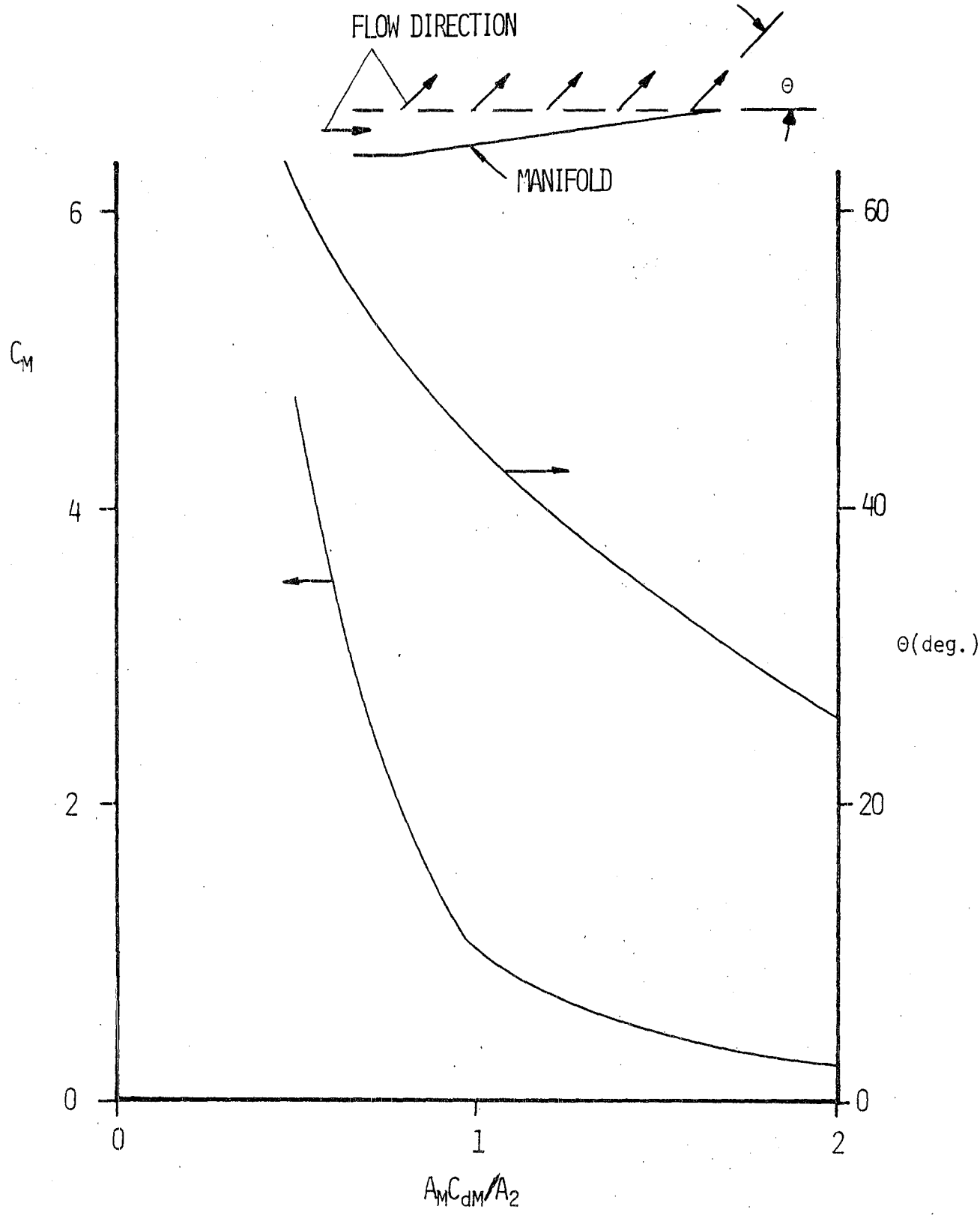

Figure 34

Manifold Loss Coefficient and Discharge Angles as a Function of Manifold Area Ratio

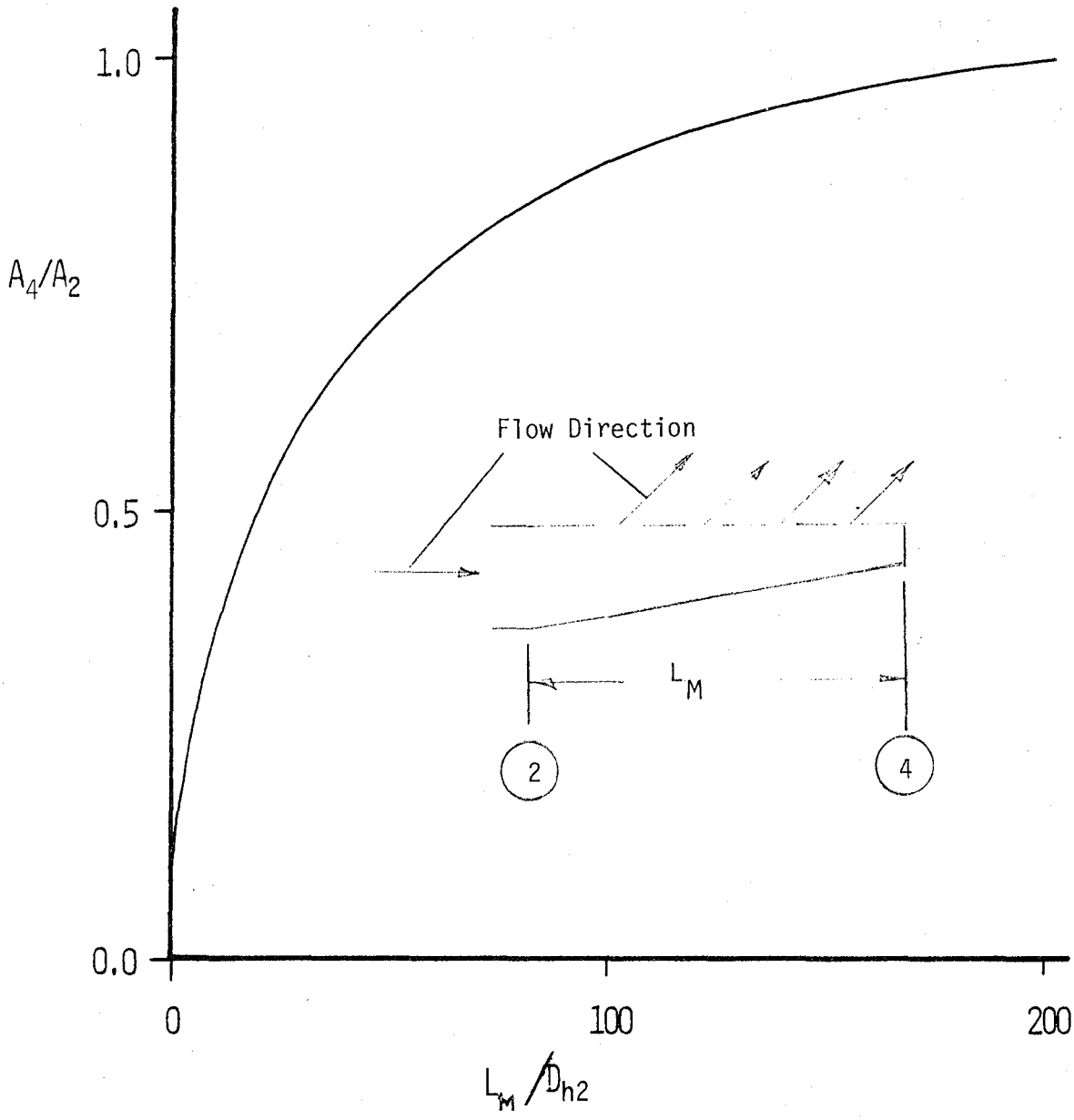

Figure 35

Manifold Taper Ratio vs. Length Ratio for a Constant Pressure Manifold

1. Report No. NASA CR-170408	2. Government Accession No.	3. Recipient's Catalog No.
4. Title and Subtitle A PRELIMINARY INVESTIGATION OF THE DRAG AND VENTILATION CHARACTERISTICS OF LIVESTOCK HAULERS		5. Report Date December 1983 6. Performing Organization Code
7. Author(s) J. A. Hoffman and D. R. Sandlin		8. Performing Organization Report No. 10. Work Unit No.
9. Performing Organization Name and Address California Polytechnic State University San Luis Obispo, California 93407		11. Contract or Grant No. NAG4-7
12. Sponsoring Agency Name and Address National Aeronautics and Space Administration Washington, D.C. 20546		13. Type of Report and Period Covered Contractor Report – Final 14. Sponsoring Agency Code RTOP 141-20-11

15. Supplementary Notes

NASA Technical Monitor: Edwin J. Saltzman, NASA Ames Research Center, Dryden Flight Research Facility, Edwards, California 93523

16. Abstract

A wind tunnel evaluation of the drag and ventilation characteristics of a conventional (unmodified) and five modified subscale model livestock haulers at 0° yaw angle has been made. The unmodified livestock hauler has a relatively high drag coefficient, and a low velocity recirculation region exists in the forward portion of the hauler. The use of a streamlined forebody and enclosed gap reduced the drag coefficient of one model by 42% and improved the rate at which contaminants can be flushed from the cargo compartment by a factor of 2.5. From the limited data obtained, any increase in the fraction of open area of the trailer sides was found to improve the trailer ventilation. The use of a ram air inlet can improve the ventilation within the hauler and remove the low velocity recirculation region at the expense of a modest increase in the truck's drag coefficient. A mathematical model for vehicles with ram air or NACA submerged inlets was developed and appears to adequately predict the ventilation characteristics of livestock haulers. In a limited study, the wind tunnel model flow patterns for an unmodified configuration appear to correspond favorably to full-scale results of an unmodified vehicle.

17. Key Words (Suggested by Author(s))	18. Distribution Statement
Livestock transportation Ventilation Aerodynamic drag Streamlining Fuel economy	Unclassified - Unlimited STAR category 85

19. Security Classif. (of this report)	20. Security Classif. (of this page)	21. No. of Pages	22. Price*
Unclassified	Unclassified	81	A05

For sale by the National Technical Information Service, Springfield, Virginia 22161.

End of Document